2020

Determination of Samarium and Dysprosium Solubility

Seana Brennan
Wilfrid Laurier University, bren5440@mylaurier.ca

Determination of Samarium and Dysprosium Solubility

by

Seana Brennan

Honours Bachelor of Science, University of Waterloo, 2014

THESIS

Submitted to the Department of Chemistry and Biochemistry Faculty of Science

in partial fulfilment of the requirements for the Master of Science in Chemistry and Biochemistry

Wilfrid Laurier University

2020

Abstract

In recent years, the use of Rare Earth Elements (REE) has rapidly increased, resulting in numerous potential anthropogenic inputs to the environment. As a result, these metals are emerging as microcontaminants and pose a potential threat to aquatic life. However, the toxicity of REE are largely unknown due, in part, to the limited information on their chemical speciation. The purpose of this project was to gain an understanding of REE precipitate formation and solubility as the foundation for the development of the chemical equilibrium component of toxicity prediction models. Solubility experiments were conducted with Samarium, (Sm), a light REE, and Dysprosium, (Dy), a heavy REE and measured using an Inductively Coupled Plasma Optical Emission Spectrometer (ICP-OES). Water chemistries of varying pH (6, 7, 8 and 9), total metal (1 μM, 10 μM and 100 μM) and total carbonate (atmospheric CO_2, 1 mM and 10 mM) were used to study the kinetics of precipitate formation over a 120-h period. Experimental results indicate that data obtained at atmospheric CO_2 and low total metal concentrations was unreliable, likely due to the difficulty in measuring solubility limits near the ICP-OES detection limit. Furthermore, most of the water chemistries explored appeared to achieve steady-state conditions within 24-h for both Sm and Dy, indicating the suitability of 24-h renewal processes used in acute toxicity tests. However, measured dissolved metal concentrations did not approach the predicted equilibrium concentrations, indicating that while steady-state conditions were achieved, equilibrium was not reached. For Sm, geochemical models over predicted the amount of precipitation for most water chemistries, with the exception of at low pH where no precipitation was predicted. The opposite trend was predicted for Dy, with over predicted precipitation at pH 8 and 9. Very little precipitation was observed under atmospheric conditions, while data for 1 mM and 10 mM total carbonate concentrations agreed strongly with one another

for all total Sm and Dy concentrations. This was an indication that the Sm or Dy available for complexation, and therefore precipitation, was in much lower concentration than carbonate. This was especially true at high pH values. All metal precipitated at pH 9 for most water chemistries. Under these conditions, the system was saturated with both hydroxides and carbonates, which provided a greater opportunity for precipitation. Future work is required to investigate the formation of multi-ligand precipitates with Sm and Dy, as well as the investigation of the role that DOM plays in precipitate formation.

Acknowledgements

When I started my master's, I thought that I was being given an opportunity to gain lab experience, learn about aquatic chemistry and add a few extra letters to the end of my name. I did not realize that I would have the opportunity to work with such an impressive, caring and kind professor who made this journey much more enjoyable for me. Thank you, Scott, for your infinite patience and understanding. You have a unique way of delivering even the sternest of messages with such kindness and consideration. I am so grateful for everything that I have learned from you. Thank you for the laughs, wisdom and baseball banter. I can't thank you enough for all you have done for me.

I would also like to thank the members of my committee, Jim McGeer and Ian Hamilton. Thank you for all of your time and effort. Your insightful questions and feedback provided so many opportunities for me to learn and grow as both a graduate student and a scientist. Thank you both for all of the knowledge that you have shared with me.

Furthermore, I would like to express my gratitude to all of the members of the C.L.E.A.R lab who have helped me along the way. Each of you has shown me the ropes in some form or another and I am thankful for your guidance and camaraderie.

I would especially like to thank Weibin "Ben" Chen and Elissa Dow. Thank you, Ben, for helping me with the geochemical modeling for my project. While your ability to use modeling software, and your chemistry knowledge are extremely impressive, the greatest thing about you is your willingness to help others. You are so generous with your time and you are always willing to answer even the silliest of my questions. Thank you for everything! Elissa, you have been an incredibly supportive and caring friend throughout this journey. Thank you for always

being there to listen to my rants and provide friendly advice. Your dry sense of humour never ceases to put a smile on my face. I could not have gotten through this without your support.

Lastly, I would like to thank my family. Thank you for encouraging me to go back to school and complete a master's degree. Thank you for convincing me that I could get through even the toughest of struggles. And, thank you for providing praise on the good days and support on the bad ones. You have always been my greatest supporters and I am extremely grateful to have you all in my life.

List of Abbreviations

BLM	Biotic Ligand Model
C_T	Total Carbonate
DOM	Dissolved Organic Matter
Dy	Dysprosium
HREE	Heavy Rare Earth Elements
ICP-OES	Inductively Coupled Plasma Optical Emission Spectrometer
K_{sp}	Solubility Product
LREE	Light Rare Earth Elements
NdFeB	Neodymium-Iron-Boron
NOM	Natural Organic Matter
PHREEQC	PH REdox EQuilibrium in C programming language
Q	Ion product
REE	Rare Earth Elements
Sm	Samarium
SmCo	Samarium-Cobalt
TMF	Toxicity Modifying Factors

List of Figures

List of Tables

Table of Contents

Chapter 1: Introduction

1.1 Rare Earth Elements

The rare earth elements (REE) are emerging as some of the most commonly found microcontaminants in the environment due to numerous anthropogenic inputs caused by their increased use (Alonso et al. 2012). The unique magnetic and luminescent properties of REE have proven to be very useful for high technology applications. Commercial products in the high technology sector, including electric and hybrid vehicles, laptop computers, LCD televisions, hard disk drives and wind turbines, are powered by permanent magnets that contain rare earths (Navarro and Zhao 2014). However, the use of these metals poses many potential threats to the environment due to the poor recyclability, unsafe mining practices and lack of understanding of their metal speciation. These topics will be explored in more detail in the following sections.

1.1.1 Lanthanides and Their Chemical Behaviour

The lanthanides are a group of 15 unique metals whose atomic numbers range from 57 to 71. REE are comprised of these 15 metals, plus Scandium and Yttrium. These metals are commonly broken into two categories: light rare earth elements (LREE) and heavy rare earth elements (HREE), based on their electron configuration (Gergoric et al. 2017). Lanthanides with unpaired *4f* electrons (La-Gd) are considered LREE, while those with paired 4*f* electrons (Tb-Lu) are categorized as HREE (Gergoric et al. 2017). The research described in this thesis will focus

specifically on a representative LREE Samarium (Sm) and a representative HREE Dysprosium (Dy).

The lanthanides are characterized by the presence of occupied *f* orbitals and typically have an oxidation state of +3 (Moeller 1970). The *f* orbital population changes for each element, but they do not participate in complexation, as their energy levels are lower than that of their outer shell (s and d) electrons. This effect contributes to the uniformity of the chemical behaviour of lanthanides (Karraker 1970).

1.1.2 REE Abundance

Despite their misleading name, REE are not actually rare. In fact, the lanthanides are more abundant in the Earth's crust than several other metals including silver, gold and platinum (EPA, 2012; Haxel, G.B. et al., 2002). The crustal abundance of several elements is summarized in Figure 1-1 (Haxel, G.B. et al., 2002). The name "rare earth elements" was devised from the difficulty in extracting REEs from alloys containing these metals (EPA 2012). Due to the chemical uniformity of REE, as described in

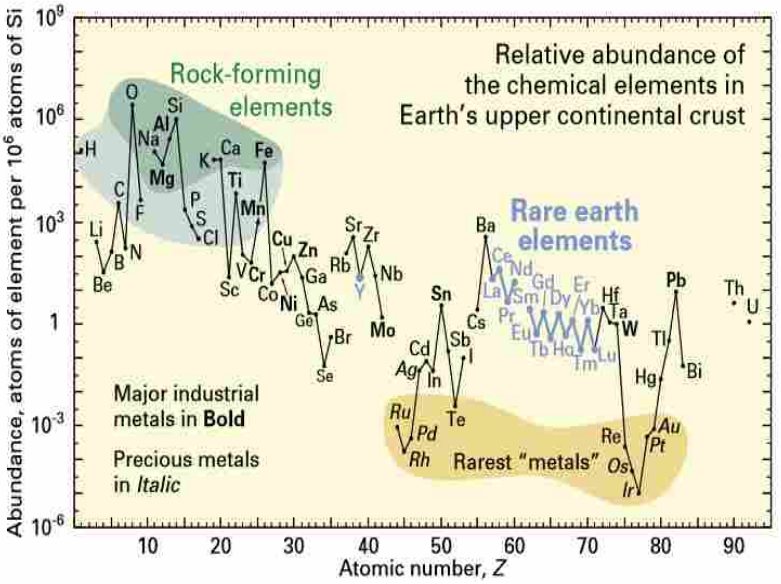

Figure 1-1: Relative abundance of several elements, including REEs (Haxel, G.B. et al., 2002).

section 1.1.1, existing technology does not allow for a single REE to be easily separated from a mixture of metals. This contributes to their "rarity" (EPA 2012).

1.1.3 Commercial Uses of REE

The lanthanides have emerged as high technology metals due to their unique magnetic, luminescent and catalytic properties (Paul and Campbell 2011). These properties have contributed to an increase in rare earth consumption in recent years, largely due to the presence of REE in products in the high technology sector (Navarro and Zhao 2014). Many commercial products including electric and hybrid vehicles, laptop computers, LCD televisions, hard disk drives and wind turbines are powered using permanent magnets that contain rare earths. As of 2016, nearly a third of global rare earth consumption was attributed to their use in permanent magnets (IMCOA 2017). This fraction is expected to rise with the continued use of permanent magnets in electronics, and the short life of high technology consumer products (IMCOA 2017). More specifically, samarium is a silvery-white metal that is predominantly used for magnets and optical lasers (ChemInfo 2012). It is used to provide resistance to demagnetization of Samarium-Cobalt (SmCo) magnets at high temperatures. These magnets are much stronger than their Neodymium-Iron-Boron (NdFeB) counterparts and have been used in the miniaturization of electronics such as headphones and stereos (Emsley 2011). Sm has also been used in the doping of calcium chloride crystals in the production of optical lasers (Emsley 2011). Dysprosium is a bright, metallic element that is rarely used in its pure metal form due to its high reactivity with water and air (ChemInfo 2012). Dy is commonly used in NdFeB permanent magnets in order to

prevent demagnetization at high temperatures (Emsley 2011). These magnets are used in electronic devices, wind turbines and electric vehicles (Emsley 2011).

1.1.4 Global Demand for REE

While the unique properties of REE have proven to be useful for many high technology applications, the growing number of commercial products that contain these metals has resulted in a significant increase in their demand. In recent years, the global demand for REE has increased dramatically, with the prediction that it will more than triple over the next 25 years (Humphries 2013). The consumption of HREE in particular has grown by several orders of magnitude in the past two decades and is expected to continue to rise with the unrelenting use of these metals (Haque et al. 2014). In order to meet the rising demand for REE and allow for the sustainable use of these metals, it will be necessary to reduce the environmental impact of rare earth mining and increase the fraction of rare earths being recycled. This will be discussed further in the following sections 1.1.5 and 1.1.7.

1.1.5 REE Mining and Associated Environmental Concerns

Although REE are not rare in their crustal abundance, the extraction of ore deposits containing these metals is restricted in many parts of the world for both economic and environmental reasons (Humphries 2013). According to a recent United States Geological Survey, the global REE deposits are sufficient to meet predicted global REE demands for the foreseeable future (Cordier and Hedrick 2008).

However, Bayan Obo in China, Mountain Pass in the United States and Mount Weld in Australia are the only currently operating REE mines, likely due to the high cost of REE mining (Cordier and Hedrick 2008). Furthermore, the global production of REE is almost completely controlled by China, with over 95% of REE mining and processing taking place at China's Bayan Obo mine (Humphries 2013; Cordier and Hedrick 2008).

Extraction of REE from ore deposits is among the most environmentally destructive and toxic of all mining practices (Gergoric et al. 2017). The water and energy consumption during REE processing is considerably higher than the amount used during the processing of other metals (Haque et al. 2014). Substantial environmental damage including landslides, clogged rivers, and pollution have resulted from REE processing and pose a threat to the health and safety of residents near China's Bayan Obo mine (Goonan 2011; Gergoric et al. 2017). Recent statistics on China's REE production within the Baotou region found that approximately ten million tons of wastewater from REE processing is produced every year, most of which is discharged without being effectively treated. This is in addition to the greenhouse gas footprint generated by the use of hydrochloric acid, steam and electricity during REE processing (Haque et al. 2014). Furthermore, about 2000 tons of mine tailings are produced with each ton of rare earth ore deposit that is processed (Gergoric 2017). For this reason, the Chinese government has restricted exports of REE since 2011, in an attempt to improve the sustainability of REE mining and production (Gergoric 2017).

1.1.6 Canada's Involvement in the REE Industry

Although China is in control of over 95% of the global production of REE, many other countries around the world contain large REE deposits (Humphries 2013; Gonzalez et al. 2015). Among them, Canada contains some of the largest HREE deposits, particularly in the Northwest Territories and Quebec (Humphries 2013). The REE deposits present in Canada are summarized in Figure 1-2. This presents an opportunity for Canada to become a dominant contributor to the rare earth industry, given the increased use of heavy rare earths, as previously discussed in section 1.1.4 (Haque et al. 2014; Humphries 2013). Plans for sustainable REE extraction have been underway since 2010, thus creating a potential for REE production in Canada in the near future (Humphries 2013).

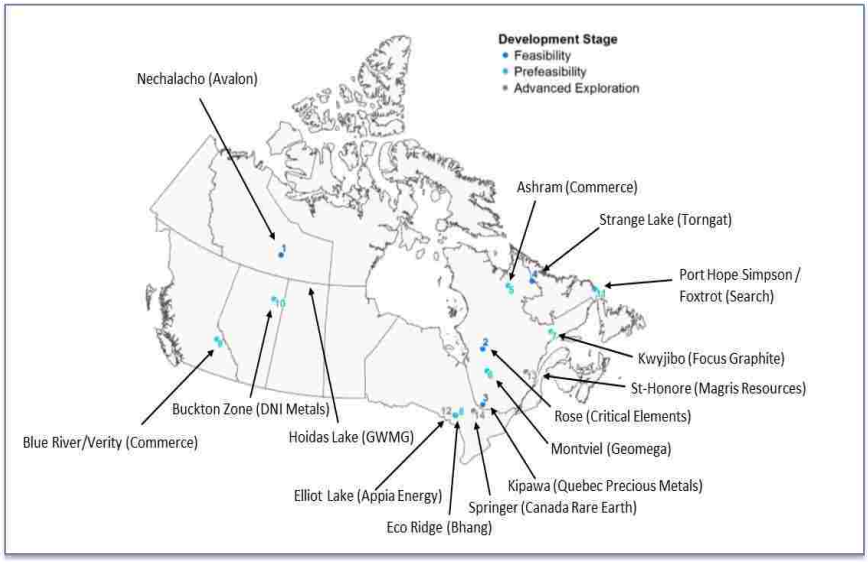

Figure 1-2: Rare earth deposits within Canada (Natural Resources Canada, 2019).

1.1.7 Poor Recyclability of REE

Despite the unique properties created by the unsaturated *4f* electrons of lanthanides, as described in section 1.1.1, it is these very properties that contribute to their poor recyclability (Gergoric 2017; Reck and Graedel, 2012). The uniformity of their chemical behaviour has resulted in a difficulty in separating any one REE from a mixture of metals. The inability to remove REE

from metal alloys has also resulted in only 1% of lanthanides being recycled from consumer products (Reck and Graedel, 2012). As such, there has been an anthropogenically driven release of REE into the environment in recent years (Goonan 2011; Gonzalez et al., 2015). These anthropogenic inputs are contributing to increases in the dissolved concentrations of REE found in aquatic ecosystems (Gonzalez et al. 2015). Though the natural dissolved concentrations of REE are reportedly only on the ng/L to μg/L scale, with Sm and Dy concentrations in Northwest Territories reported to be only 90 ng/L and 130 ng/L, respectively (Gimeno et al. 2000), these values are likely to rise with the rapidly increasing demand for REE use (Verplanck 2001; Miekeley 1992). With concentrations rising and insufficient understanding of lanthanide speciation, there is a significant urgency to determine the bioavailability and toxicity of these data poor elements.

1.2 Metal Toxicity and Speciation

In order to evaluate the toxicity of REE, it is necessary to first gain an understanding of the chemical speciation of these metals. As data poor elements, the chemical species that form between Sm and Dy and inorganic and organic ligands are not yet fully understood. As such, it is necessary to perform further research to gain insight into the chemical speciation of these metals under varied aquatic conditions. The Sm and Dy species present under various water chemistries, as well as the associated toxicity implications will be discussed in detail in the following sections.

1.2.1 Biotic Ligand Model

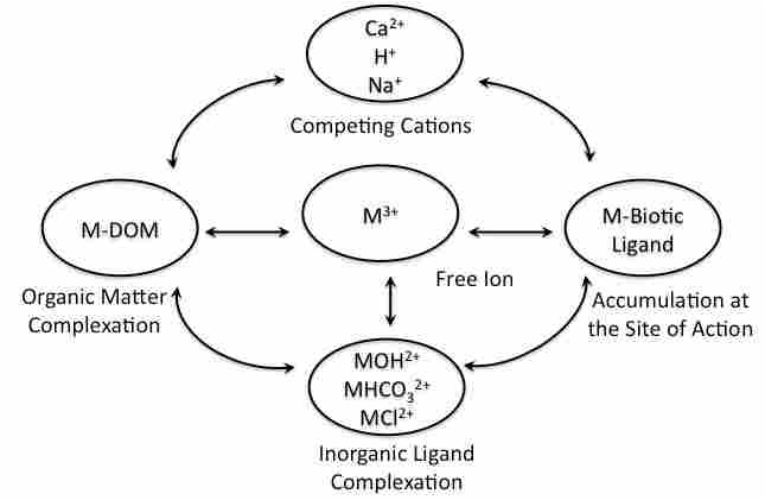

Figure 1-3: Adapted from the schematic representation of the Biotic Ligand Model found in Di Toro et al. 2001.

The Biotic Ligand Model (BLM) is a tool that has frequently been used for environmental risk assessment of metals. According to the BLM, the free ion is the most toxic species, as it is believed to be the most bioavailable form. The site of action, often the gill surface, is commonly referred to as the biotic ligand and toxicity is proportional to the accumulation of the free metal ion at the biotic ligand (Di Toro et al. 2001). There are several factors, known as toxicity modifying factors (TMF), that impact the availability of the free metal to accumulate at the biotic ligand. These factors include inorganic ligand complexation, organic matter complexation, and competing cations and are said to be protective. Inorganic ligands including hydroxide, carbonate and phosphate and organic matter are naturally available for binding, and have been known to bind to lanthanides (Sneller et al. 2000). When a metal is bound to an organic or inorganic ligand, including dissolved organic matter (DOM), it is no longer in the form of a free metal ion, and therefore cannot accumulate at the biotic ligand. As a result, there is a decreased amount of accumulation of the free metal ion at the biotic ligand, thus reducing the toxicity of the metal (Di Toro et al. 2001). Furthermore, the BLM states that competing cations such as protons, Ca^{2+} ions and Na^+ ions are protective due to the fact that they bind at the biotic ligand without toxic effects, thus limiting the number of binding sites that are available for bioaccumulation of the free ion of

toxic metals (Di Toro et al. 2001). The BLM is depicted in Figure 1-3 shown above (Di Toro et al. 2001; Figure 1-3).

1.2.2 Toxicity Modifying Factors (TMFs)

There are several factors that have an impact on the toxicity of metals, including pH, alkalinity and the presence of dissolved organic matter. Each factor will be discussed in detail below.

1.2.2.1 pH

At low values of pH, there is significant proton competition with the free metal ion for inorganic and organic ligand binding. Ligands such as organics acids, hydroxide, phosphate and carbonate are in protonated forms at low pH and are not expected to be as readily available for binding metals (Johannesson et al. 1995). This means that there is decreased ligand binding, thus resulting in increased free metal ion concentrations (Millero et al. 2009; Santore et al. 2001). As discussed in section 1.2.1, at high free metal concentrations, there is a greater opportunity for metal binding at the biotic ligand, which is proportional to toxicity. However, the high concentration of protons present at low pH can also be protective. This is because the protons can accumulate in a non-toxic manner at the biotic ligand, and therefore reduce the availability of binding sites for free metal ions (Di Toro et al. 2001).

Conversely, at high pH values, most inorganic and organic ligands are deprotonated and therefore they are available for metal-ligand complexation (Johannesson et al. 1995). When a

metal undergoes complexation with an organic or inorganic ligand, it is no longer in the free ion form, and therefore no longer bioavailable. This reduces its toxicity to aquatic life (Di Toro 2001).

1.2.2.2 Alkalinity

Alkalinity can also affect toxicity through the competition between the free metal ion and cations found in natural waters. The presence of competing cations such as sodium (Na^+), and calcium (Ca^{2+}) has proven to be protective (Di Toro 2001). This is due to the competition for binding at the biotic ligand (Di Toro 2001). The accumulation of non-toxic Ca^{2+} or Na^+ ions at the biotic ligand prevents toxic free metal ions from accumulating, which results in decreased toxicity. Additionally, under alkaline conditions, bicarbonate, carbonate and hydroxide ions are more prevalent and can bind with toxic free metal ions, resulting in reduced accumulation at the biotic ligand and therefore reduced toxicity.

1.2.3 Speciation

The chemical speciation of Sm and Dy is not well understood and there is not yet a consensus on their speciation in natural waters. Lanthanides have been shown to interact with hydroxides, carbonates and phosphates to form insoluble salts, but the chemical speciation has not yet been completely defined. For example, there is large uncertainty associated with K_{sp} values in standard databases. The documented pK_{sp} values found in the NIST database for $Sm(OH)_{3(s)}$ and $Dy(OH)_{3(s)}$ precipitates are 25.5±0.9 and 25.9±0.9, while published values for $Sm_2(CO_3)_{2\,(s)}$ and

$Dy_2(CO_3)_{3\,(s)}$ are 32.5±0.9 and 31.5±0.9, respectively (Martell and Smith 2004). As trivalent metals, Sm and Dy are expected to show chemical similarity to Al^{3+} and Fe^{3+}. However, this is merely a starting point and does not provide sufficient information to develop a quantitative geochemical model. As hydroxides and carbonates are two of the most prevalent ligands in natural waters that form solid species with lanthanides, this was a logical starting point in the development of a more accurate solubility model. Further research is needed in order to understand the chemical speciation of Sm and Dy and make predictions about the formation of potentially toxic metal species.

1.2.3.1 Data Poor Elements

Although the toxicity of many metals such as copper and lead have been studied extensively, little is known about the toxicity of lanthanides (Gonzalez et al. 2015). Due to the fact that toxicity is species dependent, as discussed in section 1.2.1, an understanding of the chemical and physical forms and speciation of Sm and Dy is necessary to determine and predict their toxicity to aquatic life (Newman and McIntosh 1991). Three documented step-wise hydrolysis constants exist for both Sm and Dy (Martell and Smith 2004). This is inconsistent with the chemical behaviour of other trivalent metals Al and Fe, which both form a fourth hydrolysis product (Rustad et al. 1999). Furthermore, other research suggests that several more complicated chemistries exist, including Sm and Dy complexes with phosphates, biphosphates, halide anions and complexes containing both hydroxide and carbonate ions (herein referred to as multi-ligand complexes) (Spahiu and Bruno 1995). There are no accepted logK values for theses complexes,

thus demonstrating the need for further research in order to establish lanthanide speciation with a higher degree of certainty (Spahiu and Bruno 1995).

1.2.3.2 Role of Solid Phases in the Environment

While the BLM is a useful tool in performing environmental risk assessment and evaluating toxicity and bioavailability, its inputs are dissolved concentrations and therefore it does not address precipitation or the role of solid phases in aquatic environments. As trivalent metals similar to Al and Fe, Sm and Dy have a tendency to precipitate in solution. Previous research suggests that Sm and Dy precipitate in the forms of $Sm(OH)_{3\,(s)}$, $Sm_2(CO_3)_{3\,(s)}$, $Dy(OH)_{3\,(s)}$ and $Dy_2(CO_3)_{3\,(s)}$, respectively (Gonzalez et al. 2015). Like many other trace metals, these metals can be expected to have poor solubility (Angel et al. 2015). This is consistent with documented pK_{sp} values for such precipitates which were 25.5±0.9, 25.9±0.9, 32.5±0.9 and 31.5±0.9, respectively. However, with the associated errors spanning almost two orders of magnitude, the application of existing pKsp values renders the prediction of precipitate formation extremely uncertain.

In environmental science, it has been determined that the total concentration is not an accurate predictor of the bioavailability or chemical lability of toxic species in soils, sediments, or aquatic environments (Traina and Laperche 1999). This is due to the presence of precipitates and minerals (Traina and Laperche 1999). Uptake of toxic chemical species typically occurs in the solution phase, and therefore the dissolved species are accepted as the toxic chemical species to pelagic organisms. Free metal ions, as well as other dissolved bioreactive forms, have the potential to disrupt biological processes (Paquin et al. 2002). Conversely, non-reactive, geochemically stable solids typically have minimal toxicity to pelagic species (Traina and

Laperche 1999). For this reason, the ability to predict the formation of Sm and Dy precipitates with a higher degree of certainty would be useful in determining the mechanism of toxicity and help to design and interpret appropriate toxicity tests.

1.3 Goals and Objectives

The overall goal of this research was to gain a better understanding of the toxicity of REE to aquatic life through the analysis of conditions affecting precipitate formation. The specific objectives are:

(1) Measurement

To improve upon the equilibrium component of existing solubility models for Sm and Dy in freshwater environments through the analysis of measured total and dissolved concentrations.

a) Analyze Sm and Dy precipitation equilibria so that more accurate K_{sp} values can be determined This will allow for more accurate predictions about when precipitation will occur and at what equilibrium concentrations.
b) Study the kinetics of precipitate formation on a time scale that is relevant to standard toxicity exposures in order to determine the time required to achieve steady-state conditions. This will determine the suitability of standard acute toxicity protocols for each of the water chemistries explored

(2) Modelling

To investigate the accuracy of existing models for Sm and Dy precipitation with ligands including hydroxide (OH^-) and carbonate (CO_3^{2-}) at various water chemistries.

(3) Toxicity and Bioaccumulation

To further our understanding of Sm and Dy solubility as a foundation for future work involving environmental risk assessment. This will ultimately allow for the determination of Sm and Dy toxicity to pelagic aquatic organisms using the BLM.

The hypotheses for these objectives are:

(1) Precipitate formation will only be favourable at high pH, high ligand concentration and/or high total metal concentrations.

(2) Precipitate formation will occur slowly and therefore the dissolved metal concentrations can be expected to decrease from 24h to 96h and decrease further from 96h to 120h. Therefore steady-state conditions will not be achieved within 24h, as is desired for the 24-h renewals of standard acute toxicity tests.

(3) Existing models will be inaccurate due to the large errors associated with documented K_{sp} values for Sm and Dy hydroxide and carbonate precipitates.

1.4 References

Alonso, E.; Sherman, A. M.; Wallington, T. J.; Everson, M. P.; Field, F. R.; Roth, R.; Kirchain, R. E. Evaluating rare earth element availability: a case with revolutionary demand from clean technologies. *Environ. Sci. Technol.* **2012**, *46*, 3406– 3414, DOI: 10.1021/es203518d.

Angel, B. M., Apte, S. C., Batley, G. E., Raven, M. D. Lead solubility in seawater: an experimental study. *Environ. Chem.* **2016**. *13*, 489-495.

ChemInfo Services Inc. 2012. Review of the rare earth elements and lithium mining sectors. Final Report. Prepared for Environment Canada. Accessed http://www.miningwatch.ca/sites/www.miningwatch.ca/files/review_of_the_rare_earth_elements_and_lithium_mining_sectors.pdf January 15, 2019.

Cordier, D.J., and Hedrick, J.B. Rare earths: U.S. Geological Survey Minerals Yearbook. **2008.** *I*, 60.1–60.15.

Di Toro, D.M., Allen, H.E., Bergman, H.L., Meyer, J.S., Paquin, P.R., Santore, R.C. Biotic Ligand Model of the acute toxicity of metals. 1. Technical basis. *Environ. Tox. Chem.* **2001**. *20*, 2383-2396.

Emsley, J. *Nature's Building Blocks: An A-Z Guide to the Elements*, 2nd ed.; Oxford University Press: New York, N.Y., 2011.

EPA (United States Environmental Protection Agency). Rare Earth Elements: A Review of Production, Processing, Recycling, and Associated Environmental Issues. Office of Research and Development. **2012.** EPA/600/R-12/575. Revised December 2012.

Accessed http://www.miningwatch.ca/files/epa_ree_report_dec_2012.pdf on January 15, 2019.

Gergoric, M., Ekberg, C., Steenari, BM. et al. J. Sustain. Metall. **2017**. *3*, 601. https://doi.org/10.1007/s40831-017-0117-5.

Gimeno Serrano, M.J.; Auque Sanz, L.F.; Nordstrom, D.K. REE speciation in low-temperature acidic waters and the competitive effects of aluminum. *Chem. Geo.* **2000.** *165,* 167-180.

Gonzalez, V., Vignati, D.A.L., Pons, M.N., Montarges-Pelletier, E., Bojic, C., Giamberini, L. Lanthanide ecotoxicity: first attempt to measure environmental risk for aquatic organisms. *Environ. Pollut*. **2015**. 199, 139-147.

Goonan, T. G. Rare Earth Elements – End Use and Recyclability. *U.S. Geological Survey* **2011**, 5011-5094.

Haque, N.; Hughes, A.; Lim, S.; Vernon, C. Rare Earth Elements: Overview of Mining, Mineralogy, Uses, Sustainability and Environmental Impact. *Resources.* **2014.** *3,* 614-635.

Haxel, G. B.; Hedrick, J. B.; Orris, G. J.; Stauffer, P. H.; Hendley, J. W. Rare Earth Elements: Critical Resources for High Technology. **2002**. *U.S. Geological Survey Fact Sheet 087-02*.

Humphries, M. Rare earth element: the global supply chain, C.R. Service, Washington, DC. **2013**.

Johannesson, K.H., Lyons, W.B., Stetzenbach, K.J., Byrne, R.H. The Solubility control of rare earth elements in natural terrestrial waters and the significance of PO_4^{3-} and CO_3^{2-} in limiting dissolved rare earth concentrations: a review of recent information. *Aquatic Geochemistry* **1995**. *1*, 157-173.

Karraker, D.G. Coordination of trivalent lanthanide ions. *Journal of Chemical Education*. **1970**. *47*, 424-430.

Martell, A.E., Smith, R.M. NIST Standard Reference Database 46. **2004**. Version 8.0, Gaithersburg, USA.

Miekeley, N., Coutinho de Jesus, H., Porto da Silveira, C.L., Linsalata, P., Morse, R. Rare-earth elements in groundwaters from the Osamu Utsumi mine and Morro do Ferro analogue study sites, Pocos de Caldas, Brazil. *J. Geochem. Explor.* **1992**. *45*, 365-387.

Millero, F.J.; Woosley, R.; Ditrolio, B.; Waters, J. Effect of ocean acidification on the speciation of metals in seawater. *Oceanography*. **2009**. *22 (4)*, 72-85.

Moeller, T. Periodicity and the lanthanides and actinides. *J. Chem. Educ.* **1970**. *47 (6)*, 417.

Natural Resources Canada. Rare earth deposits within Canada. Image presented at board meeting for Ministry of Natural Resources. **2019**. © Her Majesty the Queen in Right of Canada, as represented by the Minister of Natural Resources, 2019

Navarro, J.; Zhao, F. Life-cycle assessment of the production of rare earth elements for energy applications: a review. **2014**. *Energy Res*. Front *(2)*, 1–17.

Newman, M. C. and McIntosh, A. W. *Metal Ecotoxicology Concepts & Applications*. Lewis Publishers Inc. Chelsea, Michigan. **1991**.

Paquin, P.R., Gorsuch, J.W., Apte, S., Batley, G. E., Bowles, K.C., Campbell, P.G.C., Delos, C.G., Di Toro, D.M., Dwyer, R.L., Galvez, F., Gensemer, R.W., Goss, G.G., Hogstrand, C., Janssen, C.R., McGeer, J.C., Naddy, R.B., Playle, R.C., Santore, R.C., Scheider, U., Stubblefield, W.A., Wood, C.M., Wu, K.B. The biotic ligand model: a historic overview. *Comp. Biochem. Physiol. Toxicol. Pharmacol.* **2002**.*133*, 3- 35.

Paul, J., Campbell, G. Investigating rare earth mine development in EPA region 8 and potential environmental impacts. *United States Environmental Protection Agency, EPA*. **2011**. document-908R11003. 35pp

Reck, B.K. and Graedel, T.E. Challenges in Metal Recycling. *Sci*. **2012**. *337*, 690-695.

Rustad, J.R.; Dixon, D.A.; Rosso, K.M. Felmy, A.R. Trivalent Ion Hydrolysis Reactions: A Linear Free-Energy Relationship Based on Density Functional Electronic Structure Calculations. *J. Am. Chem. Soc.* **1999**. *121*, 3234-3235.

Santore, R.C., Di Toro, D.M., Paquin, P.R., Allen, H.E., Meyer, J.S. Biotic ligand model of the acute toxicity of metals. 2. Application to acute copper toxicity in freshwater fish and daphnia. *Environ. Tox. Chem*. **2001**. *20*, 2397- 2402.

Sneller, F.E.C, Kalf, D.F., Weltje, L., Van Wezel, A.P. **2000**. Maximum permissible concentrations and negligible concentrations for rare earth elements (REEs). National Institute of Public Health and The Environment, Report #601501011. Accessed https://www.researchgate.net/publication/27452531_Maximum_Permissible_Concentrations_and_Negligible_Concentrations_for_Rare_Earth_Elements_REEs on January 15, 2019.

Spahiu, K. and Bruno, J. A Selected Thermodynamic Database for REE to be used in HLNW Performance Assessment Exercises. *Interntl. Nuc. Info. Sys.* **1995**. *28(5)*, 1-80.

Traina, S.J. and Laperche, V. Contaminant Bioavailability in Soils, Sediments, and Aquatic Environments. *Proc. Natl. Acad. Sci.* **1999**. *96*, 3365-3371.

Verplanck, P.L., Antweiler, R.C., Nordstrom, D.K., Taylor, H.E. Standard reference water samples for rare earth elements determinations. *Appl. Geochem*. **2001**. *16*, 231-244.

Chapter 2: Methods

Previous research indicates that both Sm and Dy form precipitates with carbonates and hydroxide ions in solution (Gonzalez et al. 2015). In order to predict the parameters that affect precipitate formation with these ligands, solubility experiments were conducted at varied pH, total carbonate concentrations and total metal concentrations. The kinetics of precipitate formation were analyzed through the removal and measurement of total and dissolved sub-samples at varying time intervals. In all cases, Sm and Dy were analyzed independently. The following methodologies were used to conduct these experiments.

2.1 Hydroxide Precipitate Formation Experiments

In order to study the hydrolysis products independently, carbon dioxide was removed from the system. This was accomplished by first acidifying the ultrapure water (generated using Milli-Q® Integral ultrapure water (Type 1) system at a resistance of <18 mΩ) using a 0.1 M HNO_3 solution (prepared using OmniTrace Ultra Nitric Acid, Fisher Scientific) to ensure that all carbonate species were converted to carbonic acid. The ultrapure water was then boiled continuously for 20 minutes, to degas the solution according to Henry's law. The boiled ultrapure water was topped with argon gas and a watch glass was used to cover the mouth of the beaker during cooling. Argon gas is more dense than air, so this step is necessary to prevent carbon dioxide from re-entering the water during the cooling process. Stock solutions of 5000 μM total Sm and total Dy were prepared using $Sm_2(SO_4)_3 \bullet 8H_2O$ (Sigma Aldrich) and $DyCl_3 \bullet 6H_2O$ (Sigma Aldrich), respectively. Additions of these stock solutions were used to

prepare solutions with a range of total metal concentrations between 1 μM and 100 μM. A background electrolyte of 0.01 M KNO_3 was also added to each solution. The pH was measured prior to the start, the end, and before each sub-sample was taken. The pH was measured using a Thermo Orion 420A+ pH meter that had been calibrated using Thermo Scientific 4.01, 7.00 and 10.00 buffer solutions. For each fixed pH, the pH was corrected to the desired value using 0.01 M HNO_3 or 0.01 M NaOH following the addition of the metal. The pH was then maintained through the drop-wise addition of 0.01 M HNO_3 or 0.01 M NaOH in order to achieve a constant pH value ±0.2 for the duration of each experiment. A pair of 10 mL sub-samples, one 0.45 μm filtered and one unfiltered, were taken after 24 h, 96 h and 120 h and immediately acidified with 2% (v/v) HNO_3 (prepared using OmniTrace Ultra Nitric Acid, Fisher Scientific) to preserve their composition. The total (unfiltered) and dissolved (filtered) concentrations were determined using an Inductively Coupled Plasma Optical Emission Spectrometer (ICP-OES, Optima 8000, Perkin Elmer Inc.). The parameters of the ICP-OES analysis are summarized in section 2.3 below.

2.2 Carbonate Precipitate Formation Experiments

For experiments where carbonate complexation was analyzed, the boiling and acidification of the ultrapure water was not necessary. Additions of the Sm and Dy stock solutions were again used to reach a range of total metal concentrations between 1 μM and 100 μM. Similarly to the methods used for the hydroxide experiments, a background electrolyte of 0.01 M KNO_3 was used. For each fixed pH, the pH was again corrected to the desired value using 0.01 M HNO_3 or 0.01 M NaOH following the addition of the metal and carbonate (if applicable). The pH was then maintained through the drop-wise addition of 0.01 M HNO_3 or 0.01 M NaOH in order to achieve

a constant pH value ±0.2 for the duration of each experiment. For the experiments that were conducted at atmospheric CO_2, no further steps were taken in the preparation of the solutions. Sodium bicarbonate ($NaHCO_3$, Fisher Scientific) was added to solutions for experiments that were conducted at total carbonate concentrations of 1 mM and 10 mM. The pH was measured at the same time intervals as stated above. A pair of 10 mL sub-samples, one 0.45 μm filtered and one unfiltered, were taken after 24 h, 96 h and 120 h, in the same way as this was performed during the hydroxide experiments. Total (unfiltered) and dissolved (filtered) samples were acidified with 2% (v/v) HNO_3 (prepared using OmniTrace Ultra Nitric Acid, Fisher Scientific) and measured using ICP-OES (Optima 8000, Perkin Elmer Inc.). The parameters of the ICP-OES analysis are summarized in section 2.3 below.

2.3 Analysis

All total and dissolved samples obtained during the completion of the experiments described in sections 2.1 and 2.2 were analyzed using a Perkin Elmer Optima 8000 ICP-OES. The analysis was completed using the parameters summarized in Table 1 below.

Table 1: Parameters of ICP-OES analysis (Perkin Elmer 2013)

Parameter	**Value**
Instrument	Perkin Elmer Optima 8000 Series ICP-OES
Radio Frequency	1.2 kW
Torch	Quartz
Plasma Flow Rate	15.0 L min^{-1}
Nebulizing Gas Flow Rate	0.75 L min^{-1}
Peristaltic Pump Flow Rate	2.00 L min^{-1}
Argon Regulator	100 psi
Nitrogen Regulator	50 psi
Rinse Solution	2% HNO_3
Wavelength	**Sm** 359.260 nm, 360.949 nm, 442.434 nm
	Dy 353.170 nm, 364.540 nm, 394.468 nm

The analysis parameters were implemented by creating a method file using the WinMar 32 software. The plasma, nebulizing gas and pump flow rates were set at the values summarized in Table 1. During this process, the wavelengths were selected by choosing the top three wavelengths for each element from a drop-down menu. These 3 wavelengths were used to complete the analysis of the calibration standards. Following the calibration, the spectra were visually inspected and the wavelength with the greatest intensity and minimal noise was then chosen as the "best" wavelength for analysis. The method file was then modified to include only the "best" wavelength prior to the analysis of samples.

Measured values for total metal (unfiltered) and dissolved metal (filtered) were then used to calculate the dissolved fraction. The dissolved fraction was calculated using the following equation:

$$\%\ Dissolved\ M = \frac{Measured\ [Dissolved\ M]}{Measured\ [Total\ M]}\ x100\%$$

2.4 Modeling

Modeling can be a useful tool to determine chemical speciation of elements, including data poor elements. There are several types of geochemical and equilibrium modeling software available, including Visual minteq (Gustafsson 2014) and PH REdox EQuilibrium Modeling in C++ language (PHREEQC) (Parkhurst 1995). This software can be used to calculate the predicted equilibrium concentrations of all chemical species based on input constraints such as total elemental composition, pH, ionic strength and the expected chemical species, including solids, present in the system (Gustafsson 2014). Each type of modeling software has its own database of formation constants that act as inputs for the iterative process of determining chemical species concentrations (Bethke 1996). In this thesis, geochemical models are used to predict the solubility of rare earth elements.

2.4.1 Modeling Solid-Liquid Phase Equilibria

PHREEQC modeling can be used to predict equilibrium concentrations for aqueous systems (USGS 2017). In this case, it was assumed that the solid and liquid phases are in equilibrium with one another, i.e., the Sm (or Dy) precipitates have formed and equilibrium concentrations are fixed. It was hypothesized that the precipitation process would occur slowly and therefore steady-state conditions would not be reached within the first 24 h for both Sm and Dy.

Consequently, it was expected that the dissolved concentrations measured after 120 h would agree most strongly with the equilibrium concentrations predicted by PHREEQC software.

2.4.2 Modeling the Solubility of Sm and Dy

PH REdox EQuilibrium in C (PHREEQC) modeling software was used with the database of formation constants proposed by Spahiu and Bruno (referred to as SKB database herein) to predict the speciation of the system of interest (Spahiu and Bruno 1995). The amorphous phase of Sm and Dy hydroxide was selected, rather than the crystalline form. This modeling was used to predict the formation of Sm and Dy precipitates with inorganic ligands hydroxide and carbonate. These simulations were performed at fixed pH values of 6, 7, 8 and 9, and varied total metal concentrations and total carbonate concentrations to match the experimental range of these variables. Figures 2-1 and 2-2 below illustrate the conditions under which the Sm (or Dy) hydroxide precipitate was predicted to form.

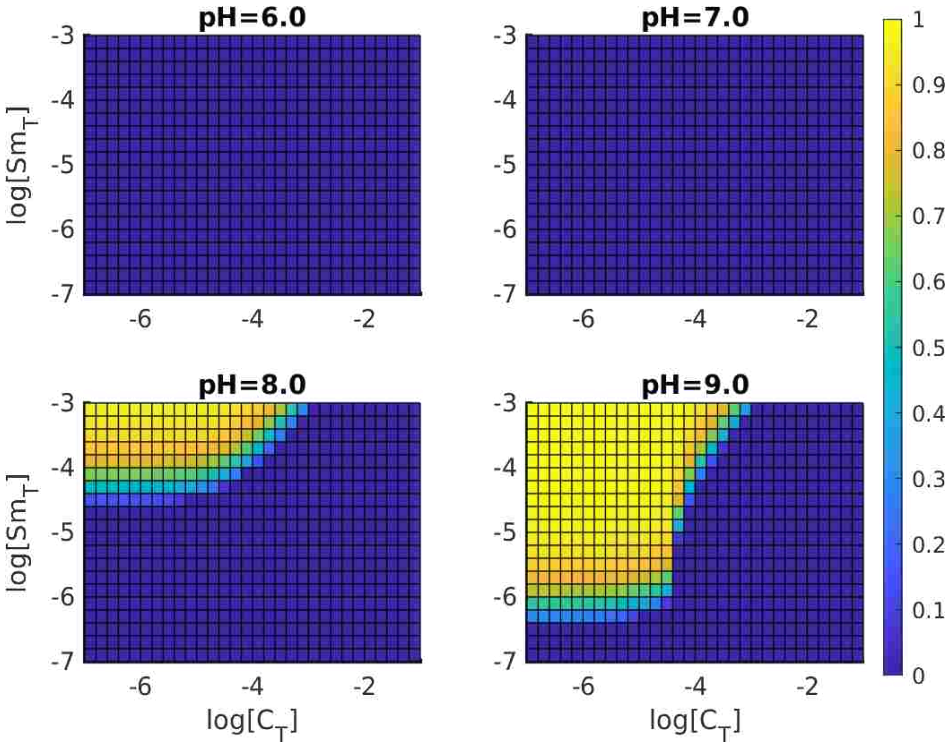

Figure 2-1: Fraction of total Sm as $Sm(OH)_3$, as a function of total Sm $[Sm]_T$, total carbonate $[C]_T$, and pH modeled in PHREEQC using SKB database; the z-axis is normalized, ranging from 0 to 1. $Sm(OH)_{3(s)}$ precipitate was not expected to form at pH 6 or pH 7 for any total carbonate concentration between 1 μM and 10 mM and any total Sm concentration between 100 nM and 1 mM. The $Sm(OH)_{3(s)}$ precipitate was likely to form at total carbonate concentrations below 1 mM and total Sm concentrations above 100 μM at pH 8, and total carbonate concentrations below 100 μM and total Sm concentrations above 1 μM at pH 9.

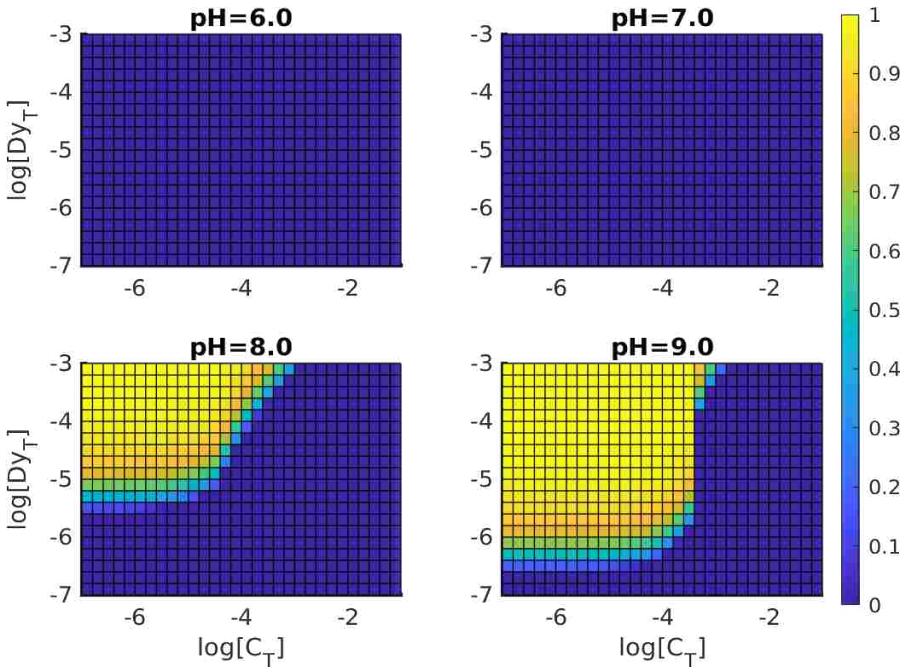

Figure 2-2: Fraction of total Dy as $Dy(OH)_3$, as a function of total Dy$[Dy]_T$, total carbonate $[C]_T$, and pH modeled in PHREEQC using SKB database; the z-axis is normalized, ranging from 0 to 1. $Dy(OH)_{3(s)}$ precipitate was not expected to form at pH 6 or pH 7 for any total carbonate concentration between 1 μM and 10 mM and any total Dy concentration between 100 nM and 1 mM. The $Dy(OH)_{3(s)}$ precipitate was likely to form at total carbonate concentrations below 100 μM and total Dy concentrations above 10 μM for pH 8, and total carbonate concentrations below 1 mM and total Dy concentrations above 1 μM at pH 9.

As is illustrated in figures 2-1 and 2-2, neither Sm nor Dy was predicted to form a hydroxide precipitate for any total metal concentration at pH 6 or pH 7, as depicted by the solid dark blue grid. This is consistent with both the low hydroxide concentrations present at these pH values, as well as the proton binding competition at low to neutral pH.

However, as the pH is increased to 8, 30-40% hydroxide precipitate formation is predicted in the range between 10 and 100 μM total Sm and total carbonate concentrations below 100 μM.

Similarly, 30-40% precipitation is expected in the range between 1 and 10 μM total Dy and total carbonate concentrations below 100 μM. Furthermore, 100% of the total Sm is expected to precipitate at total metal concentrations exceeding 100 μM and total carbonate concentrations below 1 mM. Precipitation is expected at lower total metal concentrations for Dy, with the formation of the hydroxide precipitate expected at total Dy concentrations exceeding 10 μM and total carbonate concentrations below 1 mM. Although the total carbonate concentration at pH 8 far exceeds the hydroxide concentration, the pH is below the second pK_a for carbonic acid of 10.25 (Carroll and Mather 1992), and therefore the hydroxide precipitate is much more likely to form, except in water chemistries that contain total carbonate concentrations in the millimolar range.

As the pH is further increased to 9, 100% precipitation is expected for all total Sm concentrations greater than 1 μM and total carbonate concentrations below 10 mM. In a similar fashon, 100% precipitation is expected for all total Dy concentrations greater than 1 μM and total carbonate concentrations below 1 mM. In the region where 100% hydroxide precipitate formation is predicted (shown in yellow), the total metal concentrations are on a micromolar scale, with very little free metal ion available for complexation at high pH. Thus, the 10 μM hydroxide concentration is in excess and all available metal binds to form the hydroxide precipitate. However, as the total metal concentration is increased to the millimolar range, there is more metal available for binding. The total metal concentration in this region, shown in light blue, surpasses the 10 μM hydroxide concentration, and therefore the metal cannot precipitate completely. For all pH values, Sm and Dy hydroxide precipitation predictions agree strongly.

PHREEQC was also used to predict the conditions under which Sm and Dy would form their carbonate precipitates. The results of the simulation are shown in figures 2-3 and 2-4.

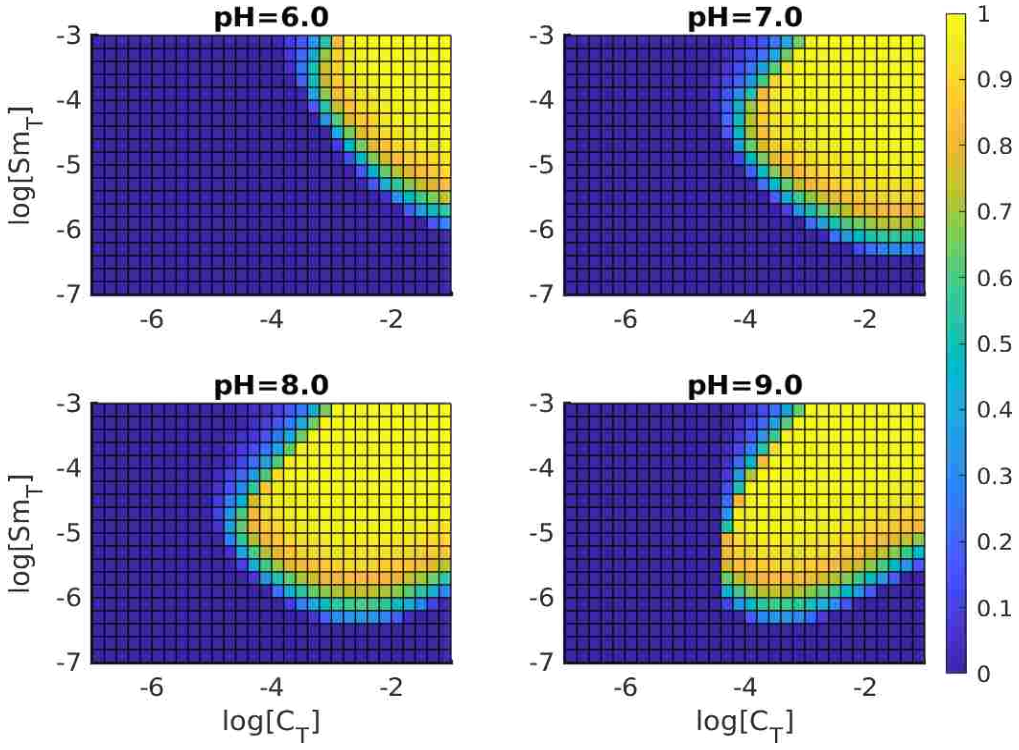

Figure 2-3: Fraction of total Sm as $Sm_2(CO_3)_3$, as a function of total Sm $[Sm]_T$, total carbonate $[C]_T$, and pH modeled in PHREEQC using SKB database; the z-axis is normalized, ranging from 0 to 1.

The $Sm_2(CO_3)_{3(s)}$ precipitate was expected to form at total carbonate concentrations above 1 mM and total Sm concentrations above 1 μM at pH 6. Similarly, formation of the carbonate precipitate was expected at total carbonate concentrations above 100 μM and total Sm concentrations above 1 μM at pH 7. The $Sm_2(CO_3)_{3(s)}$ precipitate was likely to form at total carbonate concentrations above 10 μM and total Sm concentrations above 1 μM at pH 8, and total carbonate concentrations above 100 μM and total Sm concentrations above 1 μM at pH 9.

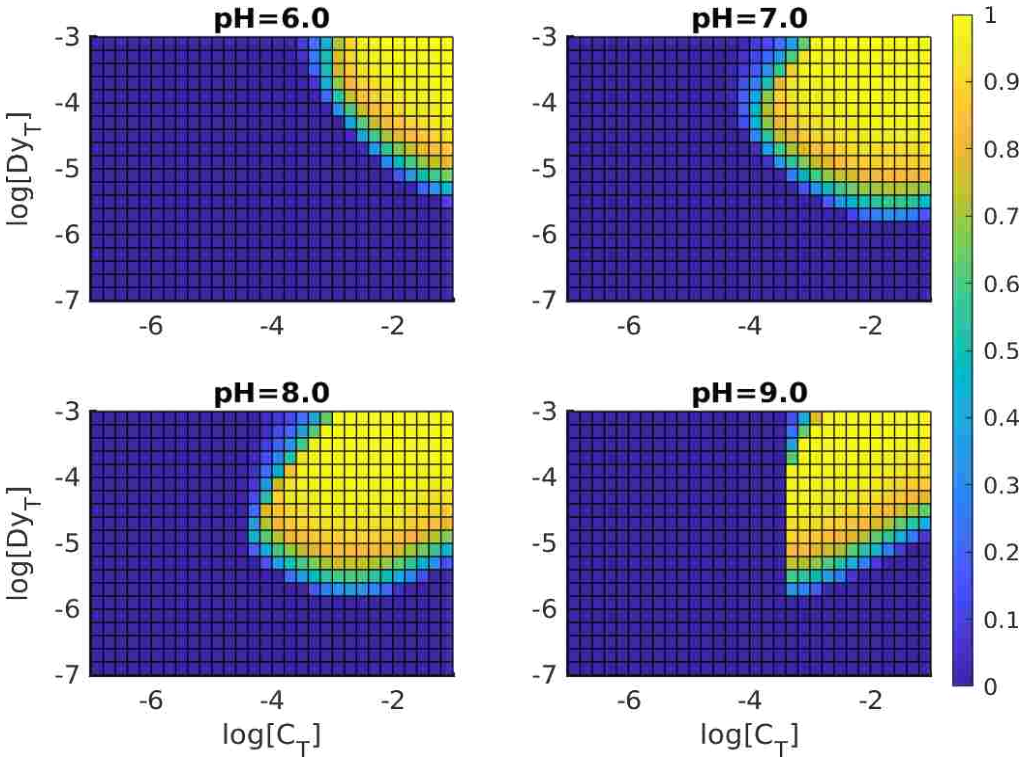

Figure 2-4: Fraction of total Dy as $Dy_2(CO_3)_3$, as a function of total Dy $[Dy]_T$, total carbonate$[C]_T$, and pH modeled in PHREEQC using SKB database; the z-axis is normalized, ranging from 0 to 1.
The $Dy_2(CO_3)_{3(s)}$ precipitate was expected to form at total carbonate concentrations above 1 mM and total Dy concentrations above 10 μM at pH 6. Similarly, formation of the carbonate precipitate was expected at total carbonate concentrations above 100 μM and total Dy concentrations above 10 μM at pH 7. The $Dy_2(CO_3)_{3(s)}$ precipitate was likely to form at total carbonate concentrations above 100 μM and total Dy concentrations above 1 μM at pH 8, and total carbonate concentrations above 100 μM and total Dy concentrations above 1 μM at pH 9.

As shown in figures 2-3 and 2-4, the precipitate formation of Sm and Dy with carbonate was not predicted to occur at pH 6 and pH 7, except in conditions where high total carbonate concentrations were present. At pH 6, carbonate precipitate formation was predicted at total carbonate concentrations above 1 mM and total metal concentrations exceeding 1 μM for both Sm and Dy.

At pH 7, Sm was expected to precipitate at total carbonate concentrations greater than 100 μM and total metal concentrations exceeding 1 μM, while Dy precipitation predictions show that the carbonate precipitate will form at total carbonate concentrations above 100 μM and total metal concentrations in excess of 10 μM. Given that the pKa_1 and pKa_2 values for carbonic acid are 6.37 and 10.25 respectively, a low carbonate concentration is expected, and therefore minimal carbonate is available for complexation at these pH values (Carroll and Mather 1992). For this reason, precipitation is only favourable at high total carbonate concentrations.

Similar trends can be observed at pH 8. However, precipitate formation is expected to occur at a lower total metal concentration and a lower total carbonate concentration for both Sm and Dy as compared to the pH 6 and 7 predictions. Precipitate formation is predicted at total carbonate concentrations above 1 mM and total metal concentrations greater than 1 μM for Sm, and total carbonate concentrations greater than 100 μM and total metal concentrations exceeding 10 μM for Dy. At pH 8, a higher percentage of the total carbonate is in the form of carbonate, although it is not the dominant carbonate species. Any carbonate ions that are available for binding are subject to competition with hydroxide ions in solution. Given that at pH 8, the hydroxide concentration is high and carbonate represents less than half of the carbonic acid species, it is logical that the formation of the carbonate precipitate would only be favourable at high total carbonate concentrations. Conversely, as the pH increases to 9, higher total carbonate and total metal concentrations are required in order for carbonate precipitate formation to be favoured. This is because the hydroxide concentration increases by an order of magnitude, while the

fraction of carbonic acid species in the form of carbonate does not increase proportionally. Thus, the carbonate precipitate is less likely to form than the hydroxide precipitate.

While this model was a good starting point and basis for the experimental design of this project, it is understood that the experimental data will be useful for the improvement of the accuracy of existing formation constants, and ultimately the model itself. This, in turn, will further understanding of the chemical speciation of Sm and Dy.

Chapter 3: Results & Discussion

3.1 Kinetics of Precipitate Formation

The experiments described in sections 2.1 and 2.2 were conducted and sub-samples were taken at time intervals of 24 h, 96 h, and 120 h, in order to study the kinetics of precipitate formation. A plateau in the slope of the data points indicates that steady state has been achieved between the solid and liquid phases of the system. It was hypothesized that precipitation would occur slowly, and therefore steady-state conditions would not be achieved within the first 24 hours for Sm or Dy for all water chemistries, as is consistent with the 24-hour renewals used during static acute toxicity tests. Equilibrium concentrations predicted using PHREEQC software are indicated using green symbols in figures 3.1 and 3.2. The data points have been connected to aid in the observation of trends in the experimental data.

The data discussed in sections 3.1.1 to 3.1.3 and plotted in figures 3.1 and 3.2 are all measured data points for t=24 h, t=96 h, and t=120 h. Figures 3-1 and 3-2 aim to analyze the kinetics of Sm and Dy precipitate formation, respectively.

3.1.1 Sm Results

Figure 3-1 below summarizes the kinetics of precipitate formation for total Sm concentrations of 1 μM to 100 μM, carbonate concentrations between atmospheric and 10 mM, and pH values 6, 7, 8 and 9. The blue lines indicate that the dissolved Sm concentration at equilibrium predicted using PHREEQC modeling software was below or equal to the dissolved Sm concentration

measured experimentally. Conversely, the red lines indicate that the PHREEQC prediction for dissolved Sm concentration at equilibrium was above the dissolved Sm concentration measured experimentally.

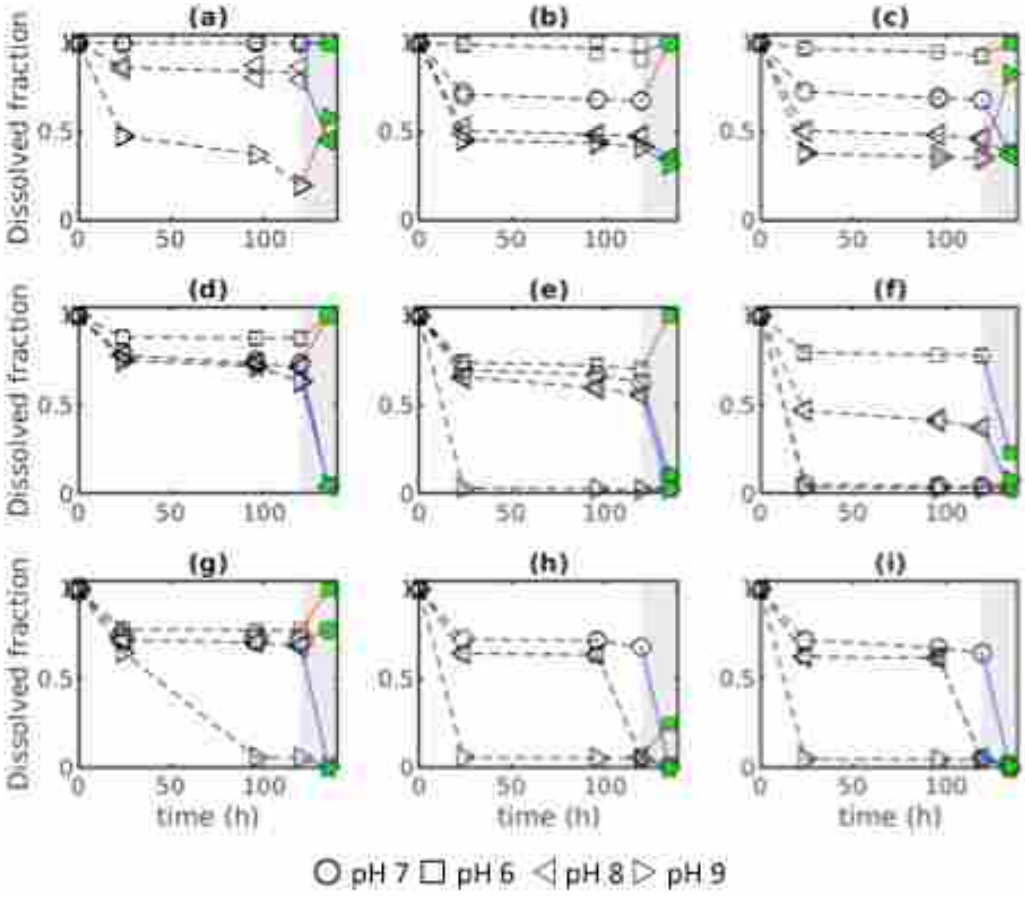

Figure 3-1: Summary of Sm kinetics data. The green symbols represent equilibrium predictions. Red lines indicate an increasing trend, while blue lines indicate a decreasing trend from the 120 hr point. (a, d, g) C_T=atm, (b, e, h) C_T=1 mM, (c,f,i) C_T=10 mM. (a,b,c) Sm_T=1μM, (d,e,f) Sm_T=10μM, (g,h,i) Sm_T=100μM. For most water chemistries, steady-state conditions were achieved within 24h, however there was a slight drop in the dissolved concentration between 96h and 120h, suggesting further precipitation. Data did not approach the predicted equilibrium concentrations for any of the water chemistries studied, indicating that steady-state conditions were achieved, but equilibrium was not reached.

In general, the blue lines follow the trends of the experimental data. The steepness of the blue lines indicates that the predicted equilibrium concentrations were substantially below the measured values. This demonstrates that the model over predicted the amount of precipitation that would occur for most water chemistries. In the rare cases when red lines were present, the pH was predominantly either 6 or 7. At these pH values, little to no precipitation was predicted, and therefore the measured dissolved Sm concentrations were below the predictions. The trends in the experimental data are discussed in more detail below.

At a total Sm concentration of 1 μM, the measured % dissolved Sm showed very little variation between data points at 24 h, 96 h and 120 h for all total carbonate concentrations and all pH values. This indicates that steady state was achieved within the first 24 h for these conditions. While the % dissolved Sm decreased with increasing pH, as expected, the kinetics of precipitate formation demonstrate that little to no further precipitation occurred beyond the first 24 h at these pH values and this total Sm concentration. The exception to this, however, was the data for pH 9 at atmospheric total carbonate. Approximately 50% of the Sm precipitated within the first 24 h, but the dissolved concentrations continued to decrease for the 96 h and 120 h data points. It is unclear if this is an indication of slow kinetics of precipitation at low total carbonate and low total Sm concentrations, or merely caused by the poor reliability of low concentration 1 μM total Sm data. The poor reliability of the data may be attributed to the close proximity to the instrument's detection limit at this concentration. Documented detection limits for the PerkinElmer Optima 8000 ICP-OES are in the low-mid ppb range (PerkinElmer 2013). Therefore the 1 μM total Sm concentration is close to, or below, the detection limit, even with

the assumption that no metal was lost to the walls of the container or sorption to the filter. This is likely a contributor to the inconsistent data.

At the lowest total Sm concentration explored, the equilibrium model predictions were highly inaccurate, with the exception of the pH 6 data. At all total carbonate concentrations, minimal precipitation was expected at pH 6, and very little precipitation was observed. The model prediction was also accurate for pH 7 under atmospheric conditions at this total Sm concentration. However, for the remaining pH values and total carbonate concentrations, the model predictions showed almost no trends. In certain instances, the model grossly overpredicted precipitation, while in others, precipitation was underpredicted. For this reason, the equilibrium modeling for 1 μM total Sm was unreliable and provided no insight into the kinetics of precipitate formation.

At a total Sm concentration of 10 μM, similar trends were observed for all pH values and all carbonate concentrations. Under these conditions, there was very little variation between the % dissolved Sm after 24 h, 96 h and 120 h, indicating that steady-state conditions were reached within the first 24 h. This shows that any precipitation that occurred was within the first 24 h, and there was minimal subsequent precipitate formation. Again, at pH 9, a decrease in the % dissolved Sm was observed for 96 h and 120 h data points, however, the decline was substantially less than that of 1 μM total Sm. The amount of Sm that precipitated increased with increasing pH, as expected. At pH 6 and 7, the dissolved fraction of Sm was greater than 80% for atmospheric and 1 mM total carbonate concentrations, indicating that these conditions are not favourable for carbonate precipitate formation. As the pH was increased to pH 8, the % dissolved

Sm decreased to between 40% and 50%, with increasing total carbonate concentration. However, at a pH of 9, all Sm precipitated within the first 24 h for total carbonate concentrations of 1 mM and 10 mM. While there is a visible difference between % dissolved Sm values at varied pH, this difference becomes significantly more noticeable with increased total carbonate concentrations. It should also be noted that the % dissolved Sm decreased with increasing carbonate concentration, as expected.

In general, the PHREEQC modeling software substantially under predicted precipitation at a total Sm concentration of 10 μM and pH 6 and 7 for all total carbonate concentrations. Conversely, for all of the explored water chemistries at pH 8 and 9, PHREEQC software predictions indicate that l00% of the total Sm will precipitate, which is a significant over prediction in most cases.

For solutions containing a total Sm concentration of 100 μM, there was little to no variability in the % dissolved Sm at 24 h, 96 h and 120 h for pH 6, 7 and 8. However, at pH 9 and atmospheric CO_2, a large decrease in % dissolved Sm was observed between the 24 h and 96 h sub-samples, followed by a plateau in % dissolved Sm between 96 h and 120 h at 0% dissolved Sm. For total carbonate concentrations of 1 mM and 10 mM, all Sm precipitated within the first 24 h at pH 9.

At the highest total Sm concentration studied, PHREEQC modeling software was the most accurate, although large discrepancies were observed at pH 7. Under atmospheric conditions, the model predicts minimal precipitation at pH 7, thus under predicting the formation of precipitates.

On the other hand, precipitation at pH 7 was overpredicted at the two higher total carbonate concentrations. At 1 mM and 10 mM total carbonate, nearly 100% precipitation was predicted at a total Sm concentration of 100 μM for all pH values. This is evidence that PHREEQC software is an inaccurate tool for predicting Sm precipitation and further research is needed to improve these geochemical models.

3.1.2 Dy Results

Figure 3-2 below is a summary of the kinetics of precipitate formation for Dy at total Dy concentrations of between 1 μM and 100 μM, carbonate concentrations between atmospheric and 10 mM, and pH values between 6 and 9. Similarly to figure 3-1, the blue lines indicate that the dissolved Dy concentration at equilibrium predicted using PHREEQC software was below the dissolved Dy concentration measured experimentally. Furthermore, the red lines indicate that the PHREEQC prediction for dissolved Dy concentration at equilibrium was above the dissolved Dy concentration measured experimentally.

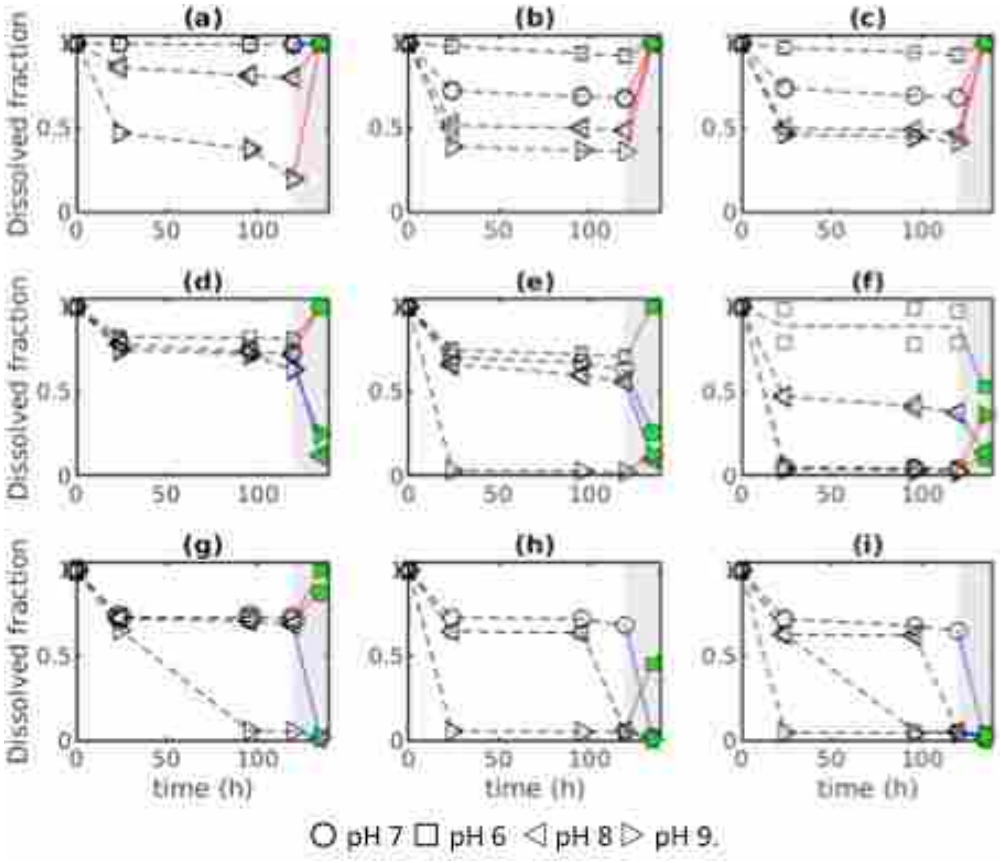

Figure 3-2: Summary of Dy kinetics data. The green symbols represent equilibrium predictions. Red lines indicate an increasing trend, while blue lines indicate a decreasing trend from the 120 hr point.
(a, d, g) C_T=atm, (b, e, h) C_T=1 mM, (c,f,i) C_T=10 mM.
(a,b,c)Dy_T=1μM, (d,e,f) Dy_T=10μM, (g,h,i) Dy_T=100μM.
For most water chemistries, steady-state conditions were achieved within 24h, however there was a slight drop in the dissolved concentration between 96h and 120h, suggesting further precipitation. Experimental data did not approach the predicted equilibrium concentrations for any of the water chemistries studied, indicating that steady-state conditions were achieved, but equilibrium was not reached.

At a total Dy concentration of 1 μM, the measured % dissolved Dy showed very little variation between data points at 24 h, 96 h and 120 h for all total carbonate concentrations and all pH values. This is an indication that steady state conditions were achieved within the first 24 h for these conditions. While the % dissolved Dy decreased with increasing pH, as expected, the

kinetics of precipitate formation show that little to no further precipitation occurred beyond the first 24 h at these pH values and this total Dy concentration. However, the exception to this trend was the data for pH 9 and atmospheric total carbonate. Approximately half of the total Dy precipitated within the first 24 h, but the dissolved concentrations continued to decrease for the duration of the 120 h period. It is unclear if this is an indication of slow kinetics of precipitation at low total carbonate and low total Dy concentrations, or merely caused by the poor reliability of 1 μM total Dy data. Similarly to what was observed with the 1 μM Sm data, the measured Dy concentrations were likely close to, or below, the instrument's detection limit. It is probable that this contributed to the poor reliability of the data.

At the lowest total Dy concentration studied, unlike the model predictions for Sm, the PHREEQC model predictions consistently under predicted the formation of precipitates. At all total carbonate concentrations and pH values, the model predicts very little precipitation. This is not what was observed experimentally. At 1 μM total Dy, for all water chemistries with a pH of 7 or higher, some precipitation was measured at each total carbonate concentration.

At a total Dy concentration of 10 μM, similar trends were observed for all pH values and all carbonate concentrations. Under these conditions, there was very little variation in the fractions of dissolved Dy after 24 h, 96 h and 120 h, indicating that steady-state conditions were reached within the first 24 h. This shows that any precipitation that occurred was within the first 24 h, and steady state conditions were achieved. Again, at pH 9, a decrease in the fraction of dissolved Dy was observed between the 96 h and 120 h data points, however, the decline was substantially less than at 1 μM total Dy. The amount of Dy that precipitated increased with increasing pH, as

expected. At pH values of 6, 7, and 8, the dissolved fraction of Dy was greater than 70% for atmospheric and 1 mM total carbonate concentrations, indicating that these conditions do not result in a large amount of precipitation. However, at a pH of 9, all Dy precipitated within the first 24 h for total carbonate concentrations of 1 mM and 10 mM. While there is a visible difference between % dissolved Dy values at varied pH, this difference becomes significantly more noticeable with increased total carbonate concentrations. It should also be noted that the % dissolved Dy decreased with increasing carbonate concentration, as expected.

In general, the PHREEQC modeling software under predicted the formation of precipitates at a total Dy concentration of 10 μM and pH 6 and 7 for all total carbonate concentrations. On the other hand, at pH 8 and 9, PHREEQC software over predicts the precipitation of the total Dy for all water chemistries.

At a total Dy concentration of 100 μM, there was little to no variability in the fraction of dissolved Dy at 24 h, 96 h and 120 h for pH 6, 7 and 8. However, at pH 9 and atmospheric CO_2, a large decrease in % dissolved Dy was again observed between the 24 h and 96 h sub-samples, followed by a plateau in fraction of dissolved Dy between 96 h and 120 h at 0% dissolved Dy. For total carbonate concentrations of 1 mM and 10 mM, all Dy precipitated within the first 24 h at pH 9.

At the highest total Dy concentration explored, PHREEQC modeling software was the most accurate. The PHREEQC predictions again under predict the formation of Dy precipitates at pH 6 and at total carbonate concentrations of atmospheric and 1 mM. However, for all water

chemistries where the total Dy concentration and total carbonate are high, the model over predicts precipitation, particularly at pH 8 and 9. This is evidence that PHREEQC software is an inaccurate tool for predicting Dy precipitation and further research is needed to improve these geochemical models.

3.1.3 Implications for Static Acute Toxicity Tests

The kinetics of precipitate formation of Sm and Dy showed strong agreement with one another. This was consistent with the chemical uniformity of the lanthanides, as well as the similarity in the values of the solubility products of these metals (Karraker 1970; Martell and Smith 2004). Experimental data indicated that steady-state conditions between solid and liquid phases were achieved within the first 24 h for most of the water chemistries explored, but equilibrium was not. For pH values of 6, 7 and 8, steady state was reached within 24 h at all total carbonate concentrations and total metal concentrations of 1 μM and 10 μM for both Sm and Dy. However, steady state was not reached within 24 h at pH 9 and/or a total metal concentration of 100 μM.

At pH 9, steady-state between the solid and liquid phases was not achieved within the first 24 h. At this pH, inorganic ligands are deprotonated and available for complexation with metal ions. The hydroxide and carbonate concentrations exceed the total metal concentrations, which results in complete precipitation of the metals. As such, minimal or no dissolved metal species exist and therefore there is no equilibration of the solid and dissolved forms. Although the inability to equilibrate within 24 h is problematic for acute toxicity tests, this pH exceeds the standard range

of pH values that are ecologically relevant and therefore would not likely be used for acute toxicity testing.

Furthermore, at a total metal concentration of 100 μM, steady state conditions were not reached within the first 24 h. At this total metal concentration, a large percentage of the metal precipitated immediately, while the remainder slowly continued to form a precipitate. Similar trends were observed by Angel et al. for a total lead concentration of 10 mg/L, where the dissolved concentration was reportedly 1.6 mg/L after 1 h and continued to decrease slowly to 1.3 mg/L (Angel et al. 2015). While this is unfavourable for 24-hour renewals of acute toxicity tests, this total metal concentration far exceeds the naturally occurring concentrations of 90 ng/L Sm and 130 ng/L Dy reported in the Northwest Territories (Gimeno et al. 2000), and therefore has limited environmental relevance.

Standard procedures for static acute toxicity tests involve the employment of a 24-h renewal process (Environment Canada, 2013). Given the fact that steady state was achieved within the first 24 h for most of the water chemistries explored, it is clear that this procedure is valid for most acute toxicity tests, assuming that test waters are left to equilibrate for 24 hours prior to organism exposure. However, in the event that the nominal concentration exceeds 10 μM total metal, it is more plausible to use a flow-through technique for acute toxicity testing. At high total metal concentrations, the solid and liquid phases do not reach steady state conditions within 24 h and the renewal is not likely to aid in the equilibration of the system. The system will ultimately remain in an unequilibrated state, giving inaccurate toxicity results. Under these conditions, it would be necessary to use a flow through technique in order to ensure that the water chemistry

remains constant for the duration of the acute toxicity test, and precipitation does not impact the efficacy of toxicity test results.

It should also be noted that at pH 8, the % dissolved metal shows a slight decrease between 96 h and 120 h for both Sm and Dy at 1 μM and 10 μM total metal and 1 mM and 10 mM total carbonate concentrations. This indicates that there is a possibility that precipitation is occurring slowly, and the system has yet to fully equilibrate. Considering that the hydrolysis of trivalent metals has proven to be a slow process (Hem and Roberson 1967), it is possible that the hydroxide precipitate was forming between the 96 h and 120 h samples, and could potentially continue to form beyond the 120 h period. This has implications for chronic toxicity tests, as equilibration would not be achieved if precipitation were continuing to occur throughout the duration of the test. It is recommended that a flow through technique be used under these conditions in order to obtain accurate chronic toxicity data.

3.2 Formation of Hydroxide Precipitates

As discussed in section 1.2.3, Sm and Dy are expected to behave similarly to other trivalent metals and form insoluble hydroxide precipitates. The formation of these hydroxide precipitates is given by the K_{sp} expression below.

$$M(OH)_{3\ (s)} \leftrightarrow {M^{3+}}_{(aq)} + 3\ {OH^{-}}_{(aq)} \qquad (1)$$

Based on the reaction given by equation (1), the ion product, Q, can be calculated for any water chemistry. The expression for calculating the ion product Q is given by:

$$Q = [M^{3+}][OH^{-}]^{3}$$

In order to predict whether precipitation is likely to occur under certain conditions, the calculated value of Q for a certain water chemistry is compared to the solubility product, K_{sp}. In the event that the value of Q exceeds the K_{sp} value, precipitation is expected to occur.

Given the high associated errors of the existing solubility products of Sm and Dy precipitates, it was expected that the following data would help to improve the accuracy of documented K_{sp} values and form the basis for more accurate solubility models.

The experimental results discussed in sections 3.2.1 and 3.2.2 are the t=120 h data points plotted on a variable-by-variable basis to aid in the visualization of trends related to total metal concentrations and pH. Although standard acute toxicity tests are 96 h in length, the 120 h data has been used for the following plots, as it was expected that this data was the closest to equilibrium conditions. As described in section 2.1, these experiments were conducted in the absence of carbonate, in order to observe the trends of precipitation with hydroxide only.

3.2.1 Sm Results

Figure 3-3 below summarizes the % dissolved Sm vs Sm_T at fixed pH values of 6, 7, 8 and 9 in the absence of carbonate. Data points have been connected to aid in the observation of trends.

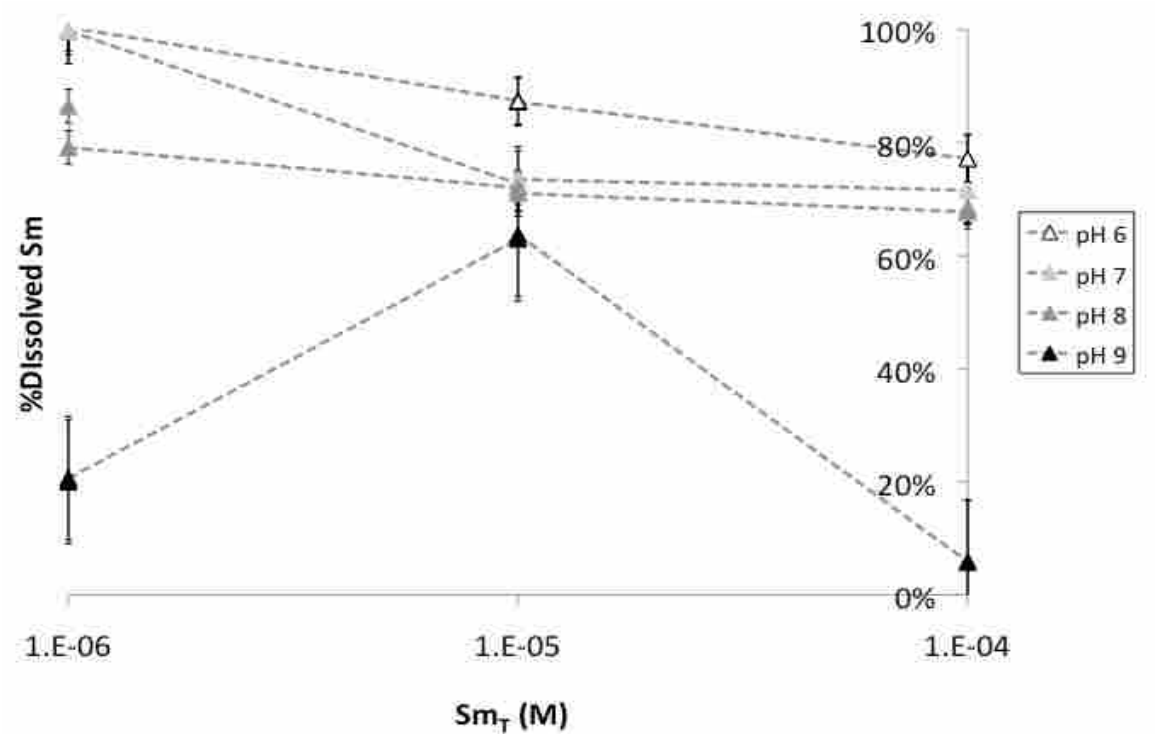

Figure 3-3: % dissolved Sm vs Sm_T at fixed pH values of 6, 7, 8 and 9. In general, the data follows the expected trend of a decreasing dissolved fraction with increasing total Sm concentration. However, the 1 μM total Sm data point at pH 9 was an apparent outlier, as it did not follow the expected decreasing trend.

As shown in figure 3-3 above, the experimental data observed for Sm complexation with hydroxide mostly follows the expected trend of increased precipitation with increasing pH and increased total metal concentration.

At a pH of 6, minimal precipitation was observed. The amount of precipitation increased from 0% to ~10% as the total Sm concentration was increased by an order of magnitude. As the total Sm concentration was further increased, the amount of precipitation also increased to ~20%. At this pH, it is expected that the free ion concentration is the highest of the pH values explored in this study. However, at this pH value, the hydroxide concentration is the lowest, compared to the

other water chemistries studied. Mathematically, the small amount of precipitation makes sense as the hydroxide concentration was only 10^{-8} M and the highest total metal concentration was only 10^{-4} M. Thus, when these concentrations are raised to their respective coefficients in the ion product expression, the result is 10^{-28} M^4, which was much smaller than the documented pK_{sp} value of 16.39. Therefore, the data follows the expected trend.

Similar trends were observed at pH 7. At a total Sm concentration of 1 µM, no precipitation was observed, as expected. While precipitation increased at 10 µM and again at 100 µM total Sm, the dissolved Sm concentrations were not below ~70%, even at the highest total metal concentration. Under these conditions, the fraction of Sm_T that is in the free ion form is less than at pH 6. However, Sm^{3+} was still expected to be the predominant species. Since the free metal ion concentration is proportional to the ion product, increased precipitation was again expected with increasing total metal concentration. However, the increase in total Sm concentration by an order of magnitude had a greater, more visible, effect due to the fact that the hydroxide concentration is higher at pH 7 than at pH 6. From a mathematical point of view, slightly increased precipitation makes sense, as the hydroxide concentration is only 10^{-7} and the highest total metal concentration is only 10^{-4} M, resulting in an ion product of 10^{-25} $M^{4.}$ While this is three orders of magnitude greater than at pH 6, the ion product is still substantially below the $10^{-16.39}$ K_{sp} value, so minimal precipitation was observed, as expected.

The experimental data obtained at pH 8 showed similar trends. However, the amount of precipitation observed at 1 µM total Sm was more than the amount measured at pH 6 or 7, as expected. Again, the increase in total Sm by an order of magnitude resulted in an increase in the

amount of precipitation by ~10%. However, the amount of precipitation appeared to plateau at approximately 30% for both pH 7 and pH 8. Given that the ion product is proportional to the total metal and there are infinite number of hydroxide ions available for precipitate formation, the amount of Sm^{3+} is likely what limited the precipitation.

At pH 9, the hydroxide concentration far exceeds the free Sm concentration. With a hydroxide concentration of 10^{-5} M and total metal concentrations ranging from 10^{-6} to 10^{-4} M, the ion product is between 10^{-21} to 10^{-19} M^4. These values are much closer to the pK_{sp} value than the ion products of the other water chemistries explored. For this reason, the likelihood of precipitation is very high, despite the relatively low Sm concentration.

3.2.2 Dy Results

Figure 3-4 below summarizes the % dissolved Dy vs Dy_T at fixed pH values of 6, 7, 8 and 9 in the absence of carbonate. Data points have been connected to aid in the observation of trends.

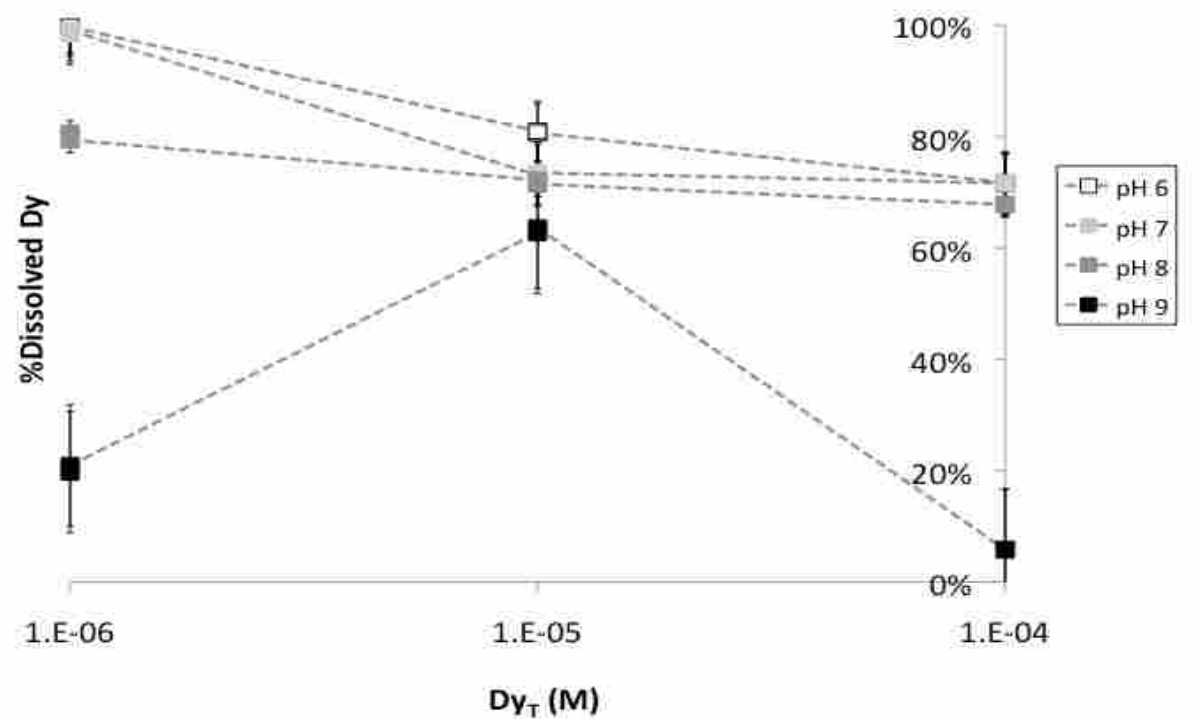

Figure 3-4: % dissolved Dy vs Dy_T at fixed pH values of 6, 7, 8 and 9. For the most part, the data follows the expected trend of a decreasing dissolved fraction with increasing total Dy concentration. However, the 1 μM total Dy data point at pH 9 was an apparent outlier, as it did not follow the expected decreasing trend.

As is illustrated by figure 3-4 above, the experimental data for Dy hydroxide precipitate formation follows the expected trend of increased precipitation with increasing pH and increased total metal concentration. The Dy results show similar trends to those observed for Sm.

At a pH of 6, minimal precipitation was observed for the lowest total Dy concentration. However, with increased total metal, the amount of precipitation increased from 0% to ~20% to ~30% with each order of magnitude increase in total Dy concentration. At this pH, it was anticipated that the Dy^{3+} concentration was the highest of the pH values explored in this study. It is also expected that the hydroxide concentration was the lowest as compared to other pH values

studied. Similarly to the Sm results, mathematically, the small amount of precipitation is logical as the hydroxide concentration is only 10^{-8} M at this pH and the highest total metal concentration is only 10^{-4} M. Therefore, when these concentrations are raised to their respective coefficients in equation (1), the resulting ion product is 10^{-28} M^4, which is much smaller than the documented pK_{sp} value of 16.09. Based on the minimal precipitation observed, it is clear that the data follows the expected trend.

The experimental data showed similar trends at pH 7. At the lowest total Dy concentration of 1 µM, no precipitation was observed, as was predicted. At this pH value, Dy^{3+} was expected to be the predominant species. Since the free metal ion concentration is proportional to the ion product, increased precipitation was again expected with increasing total metal concentration. However, the increase in total Dy concentration by an order of magnitude had a more obvious impact due to the increased hydroxide concentration at pH 7 relative to pH 6. This makes sense from a mathematical point of view, as the hydroxide concentration is only 10^{-7} and the highest total metal concentration is only 10^{-4} M, resulting in an ion product of 10^{-25} $M^{4.}$ While this is three orders of magnitude greater than at pH 7, and therefore precipitation is more likely, the ion product is still substantially below the $10^{-16.09}$ K_{sp} value, resulting in minimal precipitation.

The experimental data obtained at pH 8 showed similar trends. As anticipated, the amount of precipitation observed at 1 µM total Dy exceeded the amount measured at pH 6 or 7. Again, the increase in total Dy by an order of magnitude resulted in an increase in the amount of precipitation by ~10%. However, the fraction of dissolved Dy appears to plateau at approximately 70% for both pH 7 and pH 8. Given that the K_{sp} is proportional to the total metal

and there are infinite hydroxide ions in solution at fixed pH, the amount of Dy^{3+} is likely the cause of the limited precipitation.

At pH 9, the hydroxide concentration is substantially higher than the free Dy concentration. At this pH, the hydroxide concentration is 10^{-5} M and total metal concentrations range from 10^{-6} to 10^{-4} M. This resulted in ion product values between 10^{-21} to 10^{-19} M^4. These values are much closer to the pK_{sp} value than the ion products of the other water chemistries explored. For this reason, the likelihood of precipitation is much higher, despite the relatively low Dy concentration.

3.2.3 Comparison to Existing Solubility Models

Modeling software Visual minteq and the SKB database were used to predict the formation of hydroxide and carbonate precipitates for both Sm and Dy (Gustafsson, 2014; Spahiu and Bruno 1995). The databases for these two geochemical models are significantly different from one another. This is further evidence that Sm and Dy speciation is not well understood or defined. Table 2 and Table 3 show a comparison of the formation constants included in the database for each simulation. As shown in

Table 2: Database for modeling Sm speciation and precipitation from Visual Minteq and SKB database.

Visual Minteq		SKB Database	
Dissolved Species	**logK**	**Dissolved Species**	**logK**
$Sm^{3+} + H_2O \leftrightarrow SmOH^{2+} + H^+$	-7.84	$Sm^{3+} + H_2O \leftrightarrow SmOH^{2+} + H^+$	-7.90
$Sm^{3+} + CO_3^{2-} \leftrightarrow SmCO_3^+$	7.46	$Sm^{3+} + 2H_2O \leftrightarrow Sm(OH)_2^+ + 2H^+$	-16.50
$Sm^{3+} + 2CO_3^{2-} \leftrightarrow Sm(CO_3)_2^-$	12.53	$Sm^{3+} + 3H_2O \leftrightarrow Sm(OH)_3 + 3H^+$	-25.90
$Sm^{3+} + H^+ + CO_3^{2-} \leftrightarrow SmHCO_3^{2+}$	12.67	$Sm^{3+} + 4H_2O \leftrightarrow Sm(OH)_4^- + 4H^+$	-36.90
$Sm^{3+} + NO_3^- \leftrightarrow SmNO_3^{2+}$	0.91	$Sm^{3+} + CO_3^{2-} \leftrightarrow SmCO_3^+$	7.80
		$Sm^{3+} + 2CO_3^{2-} \leftrightarrow Sm(CO_3)_2^-$	12.80
		$Sm^{3+} + H^+ + CO_3^{2-} \leftrightarrow SmHCO_3^{2+}$	12.43
		$Sm^{3+} + NO_3^- \leftrightarrow SmNO_3^{2+}$	0.90
Solid Species	**log K_{sp}**	**Solid Species**	**log K_{sp}**
$Sm(OH)_{3\,(s)} \leftrightarrow Sm^{3+} + 3OH^-$	16.39	$Sm(OH)_{3\,(s)} \leftrightarrow Sm^{3+} + 3OH^-$	16.5
$Sm_2(CO_3)_{3\,(s)} \leftrightarrow 2Sm^{3+} + 3CO_3^{2-}$	-32.50	$Sm_2O_{3\,(s)} + 6H^+ \leftrightarrow 2Sm^{3+} + 3H_2O$	42.9
		$Sm_2(CO_3)_{3\,(s)} \leftrightarrow 2Sm^{3+} + 3CO_3^{2-}$	-34.5
		*$Sm(OH)CO_{3\,(s)} \leftrightarrow Sm^{3+} + OH^- + CO_3^{2-}$	-

*** Note: This reaction is included in the SKB database, but was not included the in geochemical modeling in this thesis due to the absence of a published K_{sp} value.**

Table 2, Visual minteq predicts very few chemical species in the complexation of Sm with hydroxide in the absence of carbonate. The only Sm species predicted to be present are Sm^{3+}, $SmOH^{2+}$ and $Sm(OH)_{3\,(s)}$. The SKB database has a much more complicated list of reactions and predicts the formation of several additional hydrolysis products, including $Sm(OH)_2^+$ and $Sm(OH)_4^-$ (Spahiu and Bruno 1995).

Similarly, Table 3 shows a database comparison of Visual minteq and SKB database for Dy. As shown, Visual minteq has a simple database for hydroxide complexation of Dy. The expected Dy species in solution in the absence of carbonate are Dy^{3+}, $DyOH^{2+}$ and $Dy(OH)_{3\,(s)}$. Other Dy species such as $Dy(OH)_2^+$ and $Dy(OH)_4^-$ listed in the SKB database are not included in the Visual minteq basis set (Spahiu and Bruno 1995). The Visual minteq database also fails to address the formation of the dissolved $Dy(OH)_3$ hydroxide complex.

Table 3: Database for modeling Dy speciation and precipitation from Visual Minteq and SKB database.

Visual Minteq		SKB Database	
Dissolved Species	**logK**	**Dissolved Species**	**logK**
$Dy^{3+} + H_2O \leftrightarrow DyOH^{2+} + H^+$	-7.59	$Dy^{3+} + H_2O \leftrightarrow DyOH^{2+} + H^+$	-7.95
$Dy^{3+} + CO_3^{2-} \leftrightarrow DyCO_3^+$	7.56	$Dy^{3+} + 2H_2O \leftrightarrow Dy(OH)_2^+ + 2H^+$	-16.20
$Dy^{3+} + 2CO_3^{2-} \leftrightarrow Dy(CO_3)_2^-$	12.91	$Dy^{3+} + 3H_2O \leftrightarrow Dy(OH)_3 + 3H^+$	-24.70
$Dy^{3+} + H^+ + CO_3^{2-} \leftrightarrow DyHCO_3^{2+}$	12.83	$Dy^{3+} + 4H_2O \leftrightarrow Dy(OH)_4^- + 4H^+$	-33.50
$Dy^{3+} + NO_3^- \leftrightarrow DyNO_3^{2+}$	0.31	$Dy^{3+} + CO_3^{2-} \leftrightarrow DyCO_3^+$	7.95
		$Dy^{3+} + 2CO_3^{2-} \leftrightarrow Dy(CO_3)_2^-$	13.20
		$Dy^{3+} + H^+ + CO_3^{2-} \leftrightarrow DyHCO_3^{2+}$	12.48
		$Dy^{3+} + NO_3^- \leftrightarrow DyNO_3^{2+}$	0.60
Solid Species	**log K_{sp}**	**Solid Species**	**log K_{sp}**
$Dy(OH)_{3\,(s)} \leftrightarrow Dy^{3+} + 3OH^-$	16.09	$Dy(OH)_{3\,(s)} \leftrightarrow Dy^{3+} + 3OH^-$	15.9
$Dy_2(CO_3)_{3\,(s)} \leftrightarrow 2Dy^{3+} + 3CO_3^{2-}$	-31.50	$Dy_2O_{3\,(s)} + 6H^+ \leftrightarrow 2Dy^{3+} + 3H_2O$	47
		$*Dy_2(CO_3)_{3\,(s)} \leftrightarrow 2Dy^{3+} + 3CO_3^{2-}$	-34
		$*Dy(OH)CO_{3\,(s)} \leftrightarrow Dy^{3+} + OH^- + CO_3^{2-}$	-

*** Note: This reaction is included in the SKB database, but was not included the in geochemical modeling in this thesis due to the absence of a published K_{sp} value.**

It should also be noted that the pK_{OH} values for Sm and Dy contained in the SKB database do not strongly agree with one another. These metals react according to equations (2), (3), (4) and (5) shown below.

$$M^{3+} + H_2O \leftrightarrow MOH^{2+} + H^+ \quad (2)$$

$$M^{3+} + 2H_2O \leftrightarrow M(OH)_2{}^{+} + 2H^{+} \quad (3)$$

$$M^{3+} + 3H_2O \leftrightarrow M(OH)_3 + 3H^{+} \quad (4)$$

$$M^{3+} + 4H_2O \leftrightarrow M(OH)_4{}^{-} + 4H^{+} \quad (5)$$

For Sm, the step-wise hydrolysis constants are 7.90, 8.60, 9.40, and 11.0, while the Dy constants are 7.95, 8.25, 8.5, and 8.8 (Spahiu and Bruno 1995). These values show dissimilarity, which is unexpected, as the lanthanides are expected to have chemical uniformity (Karraker 1970).

In addition to the inconsistency of the hydrolysis constants, it has been proposed that solid multi-ligand complexes $Sm(OH)CO_{3\,(s)}$ and $Dy(OH)CO_{3\,(s)}$ form, but formation constants for these precipitates have not been determined, as indicated in tables 2 and 3 (Spahiu and Bruno 1995). In the absence of formation constants, these multi-ligand complexes cannot be added to database used for geochemical modeling. This information would be highly useful to determine whether discrepancies between experimental data and existing geochemical models can be attributed to the formation of these multi-ligand complexes.

This is evidence that further research is needed to define the chemical speciation of these data poor elements.

3.2.4 Environmental Relevance

Although hydroxide precipitation data provides useful information for the potential improvement of existing K_{sp} values for Sm and Dy hydroxide precipitates, this system is very simple and does

not have much environmental relevance. In the absence of other deprotonated ligands or free metal ions, the competition for binding that would occur naturally cannot be observed. Furthermore, in freshwater, the concentration of hydroxide ions is minimal, relative to the concentration of carbonic acid species (Carroll and Mather 1992). At neutral pH, the hydroxide concentration is below 1 μM, which is several orders of magnitude below the naturally occurring concentrations of carbonic acid species (Carroll and Mather 1992). Thus, the observed hydroxide complexation is unlikely to occur in freshwater, given that Sm and Dy are trace metals and naturally occurring hydroxide concentrations are so low. Additionally, these experiments did not include DOM that would be present in freshwater. According to the BLM, dissolved organic matter can bind to free metal ions in solution, thus limiting their bioavailability (Di Toro et al. 2001). In freshwater, DOM would compete with hydroxide ions to bind to Sm^{3+} and Dy^{3+} ions, and therefore would reduce the amount of precipitation. This, in turn, increases their solubility. For these reasons, the hydroxide precipitation experiments are not environmentally relevant.

3.3 Formation of Carbonate Precipitates

Carbonic acid species exist naturally in freshwater in the forms of H_2CO_3, HCO_3^-, and CO_3^{2-}, and are in much higher concentrations than hydroxides and protons (Carroll and Mather 1992). Carbonate readily precipitates with metals such as calcium and the alkaline earth metals (Lide 1991). Furthermore, optimum carbonate precipitation is expected to occur at a lower pH than the formation of hydroxide precipitates (Patterson et al. 1977). The carbonate precipitate forms according to the K_{sp} expression shown below.

$$M_2(CO_3)_{3\ (s)} \leftrightarrow 2M^{3+}{}_{(aq)} + 3\ {CO_3}^{2-}{}_{(aq)} \quad (6)$$

Using the reaction given in equation (6), the ion product, Q, can be calculated for any water chemistry. The expression for calculating the ion product Q is given by:

$$Q = [M^{3+}]^2[{CO_3}^{2-}]^3$$

In order to predict whether the carbonate precipitate is likely to form under certain conditions, the calculated value of Q for a certain water chemistry is compared to the solubility product, K_{sp}. In the event that the value of Q exceeds the K_{sp} value, precipitation is expected to occur.

Given the high associated errors of the existing solubility products of Sm and Dy precipitates, the experimental data will be useful in the improvement of documented K_{sp} values and form the basis for more accurate solubility models.

The experimental results in sections 3.3.1.1 and 3.3.1.2 are the t=120 h data points plotted on a variable-by-variable basis to aid in the visualization of trends related to pH.

3.3.1 The Role of pH on Precipitate Formation

The experiments described in section 2.2 were conducted at fixed pH values of 6, 7, 8 and 9 to examine the effect of pH on precipitate formation. It is expected that with increasing pH, precipitation will be more favourable. As the pH increases, so does the concentration of deprotonated ligands. This means that ligand binding is more likely to occur, resulting in increased precipitation.

3.3.1.1 Sm Results

Figure 3-5 below summarizes the % dissolved Sm at pH values between 6 and 9 and fixed total carbonate concentrations of atmospheric CO_2, 1 mM and 10 mM. Data points have been connected to aid in the observation of trends.

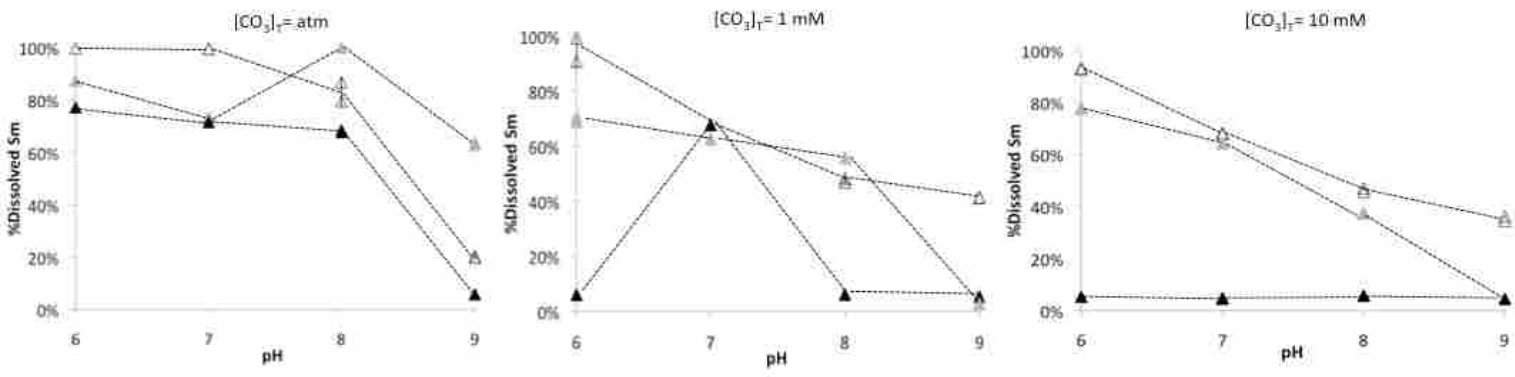

Figure 3-5: % dissolved Sm vs pH at fixed total carbonate concentrations of atmospheric CO_2, 1 mM and 10 mM.
In general, the experimental data follows the expected trend of decreasing dissolved Sm fractions with increasing pH and increasing total carbonate concentrations. However, there was an apparent outlier observed at pH 7 and 1 mM total carbonate for the highest total metal concentration studied.

At atmospheric CO_2, very little difference can be seen between the dissolved Sm concentrations for pH values of 6, 7 and 8 at all total metal concentrations. Although there was a slightly increasing amount of precipitation with increasing total Sm concentrations, the trends were similar. With the exception of the apparent outlier at pH 7 and 10 μM total Sm, the dissolved Sm concentrations were relatively constant between pH 6 and 7 and decreased by only ~10% at pH 8. Given that all total metal concentrations explored are on a micromolar scale, and the carbonate

concentration can be expected to be very low at pH values below the pK_a values for carbonic acid of 6.37 and 10.25 (Carroll and Mather 1992), it is logical that minimal precipitation was observed. From a mathematical perspective, the ion product is proportional to both the free metal ion concentration and the carbonate concentration, thus when these small numbers are raised to their respective coefficients, the result was below the pK_{sp} of -32.5. However, as the pH was increased to 9, the measured fraction of dissolved Sm was substantially decreased, as expected. Although the free ion concentration of Sm can be expected to be reduced at pH 9, the carbonate concentration is significantly higher than at pH values of 6 through 8, as this pH is approaching the second pK_a value of carbonic acid. Therefore, the net result is an increased ion product, resulting in higher probability of precipitation. A similar trend was observed for all total Sm concentrations, with 80%, 30% and 100% precipitation being measured for total Sm concentrations of 1 μM, 10 μM, and 100 μM, respectively.

Though the overall trends were similar, the reliability of the 1 μM data is questionable, considering the heightened impact of metal lost to the walls of the container or sorption to the filter at low total metal concentrations, as well as the proximity to instrumental detection limits. Overall, the experimental data obtained at a total carbonate concentration of atmospheric CO_2 indicates that there is an insufficient amount of carbonate for precipitate formation to be favourable, except at the highest total metal concentration and a pH of 9. This data provides very little information about the carbonate precipitation with Sm.

The expected trends are much more evident at 1 mM total carbonate. The fraction of dissolved Sm decreases with increasing pH, as expected. Despite the decrease in free Sm ions with

increasing pH, the ion product and therefore the probability of precipitation increases with increasing pH due to the larger fraction of carbonic acid species in the form of carbonate. Therefore, more precipitation can be expected at all pH values. This trend is illustrated by the 1 μM data with dissolved Sm fractions decreasing from 90%, to 70%, to 50%, to 30% as the pH increases from 6, to 7, to 8, to 9, respectively. These points follow a smooth, decreasing curve with increasing pH, as expected. Similar trends were observed for the 10 μM Sm_T data points at pH values of 6 through 8. The percent dissolved Sm decreases from 80% to approximately 60% as the pH increases from 6 to 7. The percent dissolved Sm decreases further to 40% at a pH of 8. However, at a pH of 9, there is a significant drop in the fraction of dissolved Sm and it approaches zero. At the highest total metal concentration of 100 μM Sm_T, it appears that all metal precipitated at all pH values, though the pH 7 data is an apparent outlier.

The Sm data obtained at 10 mM total carbonate shows a lot of similarities to the data for 1 mM C_T, excluding the previously mentioned outlier. The 1 μM and 10 μM Sm_T data follow the expected shape of a smooth decreasing solubility curve. As with the 1 mM C_T data, all points corresponding to the highest total metal concentration show 100% precipitation. The data obtained at a total carbonate concentration of 10 mM shows that the added sodium bicarbonate is in excess. At even the highest total Sm concentration of 100 μM, the total carbonate concentration is three orders of magnitude higher. Therefore, the system can be expected to run out of metal available for precipitation before all of the carbonate ions have been complexed. Since the data strongly agrees with experimental data obtained at 1 mM C_T, and the carbonate concentration far exceeds even the highest total metal concentration, it is clear that the amount of precipitation is determined by the amount of Sm and not the amount of carbonate.

3.3.1.2 Dy Results

Figure 3-8 below summarizes the % dissolved Dy at pH values between 6 and 9 and fixed total carbonate concentrations of atmospheric CO_2, 1 mM and 10 mM. Data points have been connected to aid in the observation of trends.

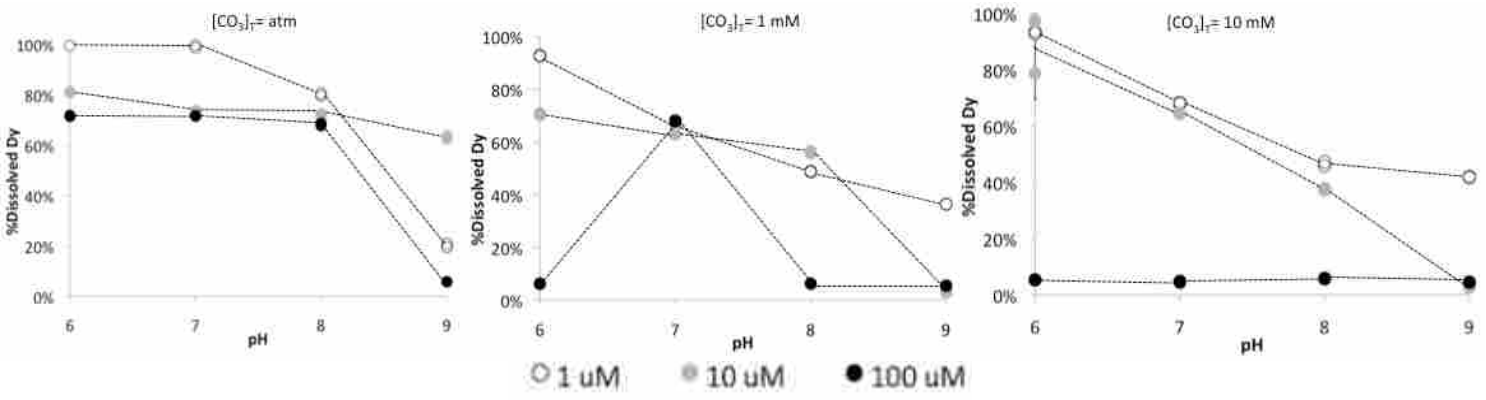

Figure 3-6: % dissolved Dy vs pH at fixed total carbonate concentrations of atmospheric CO_2, 1 mM and 10 mM.
In general, the experimental data follows the expected trend of decreasing dissolved Dy fractions with increasing pH and increasing total carbonate concentrations. However, there was an apparent outlier observed at pH 7 and 1 mM total carbonate for the highest total metal concentration studied.

Under atmospheric conditions, there is very little variation in the dissolved Dy concentrations for pH values of 6, 7 and 8 at all total metal concentrations. The experimental data for total Dy concentrations of 10 μM and 100 μM follow an approximately horizontal line, indicating a constant dissolved Dy fraction at these total metal concentrations and pH values. The 1 μM data follows a similar trend at pH 6 and 7, followed by a decrease in the dissolved fraction by ~20%. However, it is unclear whether the decrease in % dissolved Dy can be attributed to precipitation

or to the loss of metal to the walls of the container and filter. Given that all total metal concentrations explored are on a micromolar scale, and the carbonate concentration can be expected to be very low at pH values below the pK_a values for carbonic acid of 6.37 and 10.25 (Carroll and Mather 1992), it makes sense that limited precipitation was observed. Mathematically, the ion product is proportional to both the free metal ion concentration and the carbonate concentration, thus when these small numbers are raised to the corresponding coefficients, the result was below the pK_{sp} of -34.5. However, at pH 9, the measured fraction of dissolved Dy decreased considerably. As the pH approached the second pK_a value of carbonic acid, the concentration of increases, resulting in a substantial increase in ion product relative the K_{sp}. Therefore, it was expected that further precipitation would occur, given the increased carbonate. This trend was observed for all total Dy concentrations, with 80%, 30% and 100% precipitation being measured for total Dy concentrations of 1 μM, 10 μM, and 100 μM, respectively.

The expected trends were much more visible at 1 mM total carbonate. The amount of precipitation increased with increasing pH, as expected. Despite the decrease in free Dy ions with increasing pH, the ion product increases with increasing pH due to the larger fraction of carbonic acid species in the form of carbonate. Therefore, the likelihood of precipitation is increased with increasing pH. This trend can be observed in both the 1 μM and 10 μM total Dy data sets. In both cases, the fraction of dissolved Dy decreased gradually between pH values of 6 and 8, although the 1 μM data has a much steeper decline in this range. However, at a pH of 9, there was a significant drop in the fraction of dissolved Dy and it approaches zero. Furthermore, at the highest total Dy concentration of 100 μM, all metal precipitated at all pH values, though

the pH 7 data appears to be an outlier. The Dy data obtained at a total carbonate concentration of 1 mM shows that the added sodium bicarbonate provides a sufficient amount of carbonate for Dy to form precipitates at all pH values between 6 and 9. As expected, increased total metal concentrations and increased pH result in a greater amount of precipitation.

The experimental data obtained at 10 mM total carbonate is highly similar to the data for 1 mM C_T. The 1 μM and 10 μM Dy_T data follow the expected shape of a relatively smooth decreasing solubility curve. Similar to the 1 mM C_T data, all points corresponding to the highest total Dy concentration show complete precipitation. The experiments conducted at a total carbonate concentration of 10 mM show that the added sodium bicarbonate is an excess reagent. Given that the data strongly agrees with experimental data obtained at 1 mM C_T, and the carbonate concentration is significantly higher than the highest total metal concentration, it is clear that the amount of precipitation is determined by the amount of free Dy available for binding and not the amount of carbonate.

3.3.2 The Role of Carbonate Concentration on Precipitate Formation

The experiments described in section 2.2 were conducted at atmospheric CO_2, 1 mM, and 10 mM total carbonate concentrations to examine the effect of ligand concentration on precipitate formation. It was expected that with increasing ligand concentration, the formation of carbonate precipitates would occur more frequently. The pK_a values for carbonic acid are 6.37 and 10.25 (Carroll and Mather 1992)**,** thus bicarbonate is the dominant species at neutral pH and carbonate dominates in highly alkaline conditions. Given the low percentage of the carbonic acid species that is in the form of carbonate at the pH values studied, increased total carbonate concentrations

allow for the presence of carbonate ions in solution at pH values where this chemical species makes up a minimal fraction.

3.3.2.1 Sm Results

Figure 3-7 below summarizes the % dissolved Sm vs C_T at fixed pH values of 6, 7, 8 and 9.

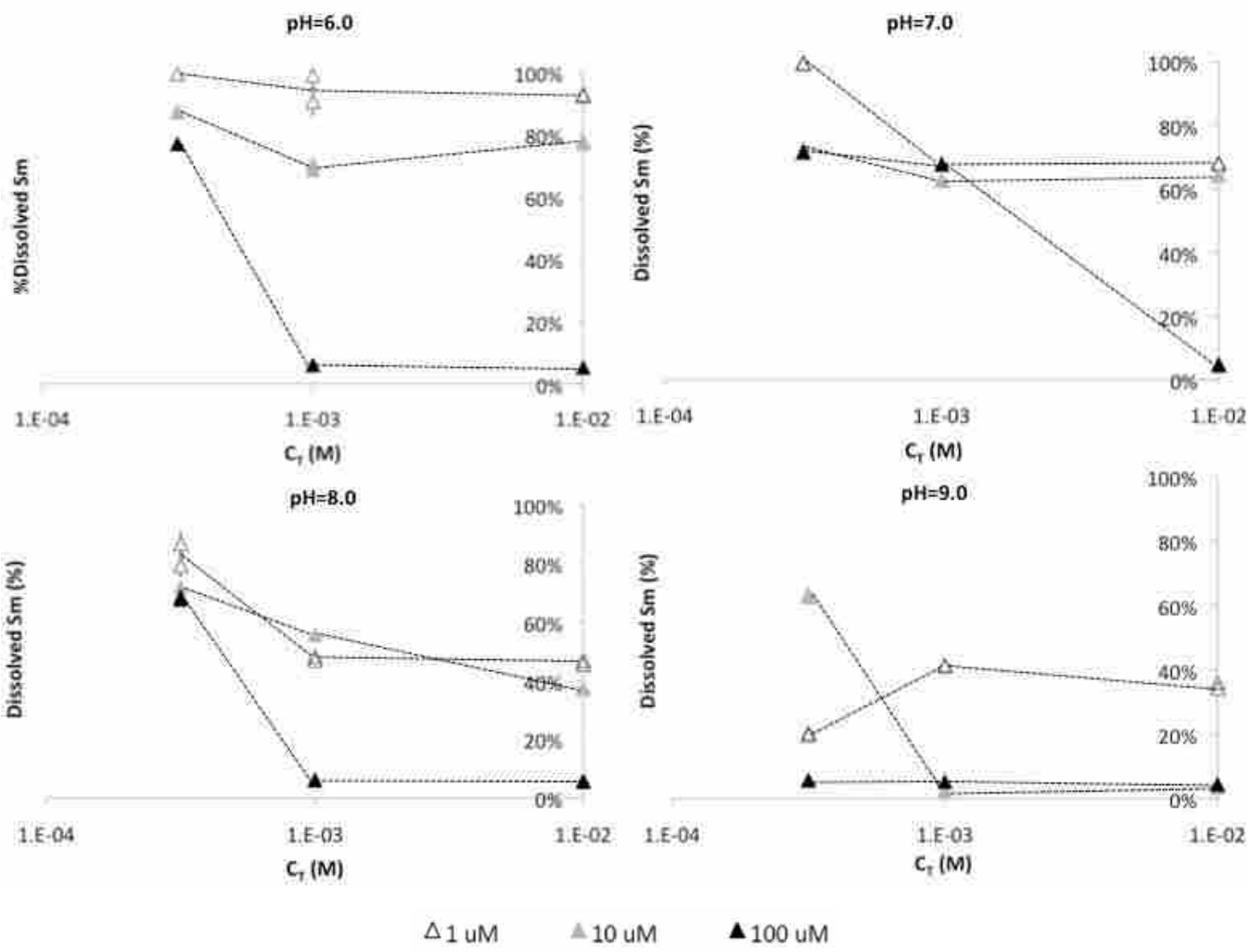

Figure 3-7: % dissolved Sm vs C_T at fixed pH values of 6, 7, 8 and 9.
As expected, experimental data show a decrease in the dissolved fraction with increasing total carbonate concentrations. This is especially visible at higher total Sm concentrations.

As shown in figure 3-7 above, very little precipitation occurred under atmospheric conditions. Carbon dioxide can exist in both gaseous and dissolved forms (Reid et al. 1987). Under atmospheric conditions of 20 ℃ and a partial pressure of CO_2 at 1 bar, the solubility of CO_2 is 0.88 cm^3/g water (Physical and Engineering Data 1978). Experiments were conducted at an ambient temperature of approximately 25 ℃. Therefore, very little dissolved CO_2 can be expected to be in solution, resulting in very low concentrations of carbonic acid species. Additionally, the total metal concentrations studied in this thesis were on a micromolar scale. Considering that the ion product is proportional to both the carbonate concentration and the free Sm ion concentration, very little precipitation is expected. This trend can be observed in figure 3-7 above. At 1 µM total Sm, almost no precipitation was observed for pH values of 6 through 8 under atmospheric conditions. Similar trends were detected at total Sm concentrations of 10 µM and 100 µM and pH 6. However, at pH 7 and 8, the 10 µM and 100 µM data appear to converge to approximately 30% precipitation. This is likely an indication that at atmospheric CO_2, the amount of carbonate available for binding is the limiting condition affecting precipitation.

The addition of 1 mM total carbonate to the system had a significant impact on the amount of precipitation observed, especially at high pH. Although the 1 µM total Sm data is again highly unreliable, the increase in the total carbonate concentration to 1 mM resulted in ~10% more precipitation at 10 µM total Sm for pH values 6 through 8, and 100% precipitation at pH 9. The impact of the increase in the total carbonate concentration was more obvious at 100 µM total Sm, as 100% precipitation was observed at all pH values, with the exception of the previously mentioned outlier at pH 7. Given that the ion product is proportional to the free Sm ion concentration and the carbonate concentration, it is logical that the increased C_T resulted in a

higher probability of precipitation, particularly at the highest total Sm concentration. Since the total Sm concentrations studied are orders of magnitude below the total carbonate concentration in the system, it is likely that all free metal will be complexed before all available carbonate ions have complexed.

As previously discussed, the data observed at 10 mM total carbonate was very similar to what was observed at 1 mM C_T for all total Sm concentrations and pH values. This is likely an indication that the added sodium bicarbonate causes carbonate and bicarbonate ions to be in excess in the system. Given that the total Sm concentrations of interest were on a micromolar scale, the amount of free metal available for binding was substantially less than the number of carbonate ions available for precipitation at this total carbonate concentration. Therefore, there is minimal change in the data despite the increase in total carbonate concentration.

3.3.2.2 Dy Results

Figure 3-8 below summarizes the % dissolved Dy vs C_T at fixed pH values of 6, 7, 8 and 9.

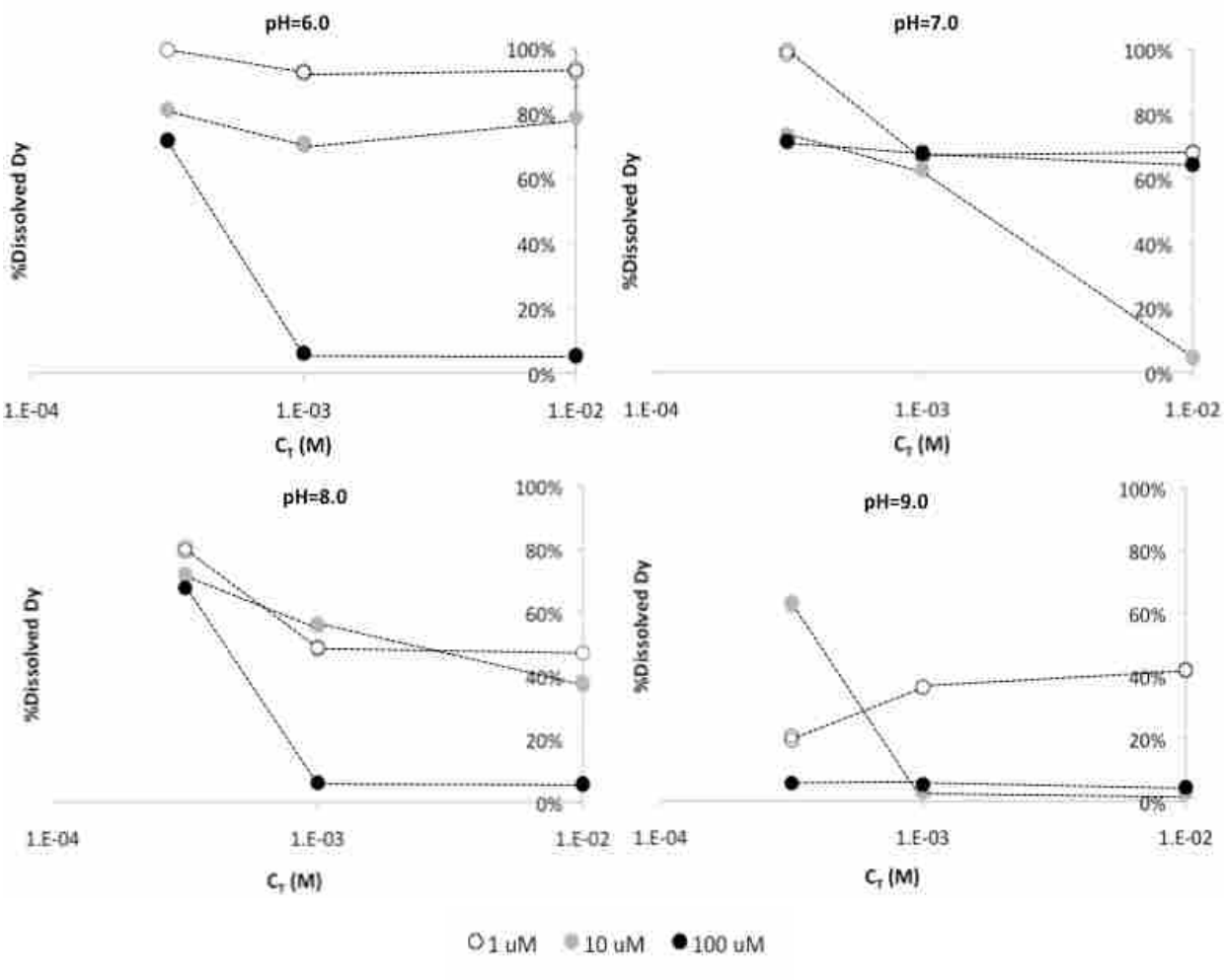

Figure 3-8: % dissolved Dy vs C_T at fixed pH values of 6, 7, 8 and 9. As expected, experimental data show a decrease in the dissolved fraction with increasing total carbonate concentrations. This is especially visible at higher total Dy concentrations.

As shown in figure 3-8 above, limited precipitation occurred under atmospheric conditions, especially at low pH and/or low total Dy. As discussed in section 3.3.2.1, carbon dioxide has poor solubility under ambient conditions, thus resulting in low dissolved concentrations of carbonic acid species. Due the proportionality of the free Dy concentration and carbonate concentrations to the ion product, very little precipitation is expected. This trend was observed in figure 3-8. At a total Dy concentration of 1 µM, almost no precipitation was observed for pH

values of 6 through 8 under atmospheric conditions. Slightly increased precipitation occurred at total Dy concentrations of 10 µM and 100 µM and pH values between 6 and 8. Approximately 20-30% precipitation was observed at 10 µM and 100 µM total Dy concentrations. The data obtained at pH 9 and atmospheric conditions, however, does not follow the same trend. Although the 1 µM total Dy data does not follow the expected trend, the 10 µM and 100 µM total Dy data do not converge as they did at lower pH values. The 10 µM data remained at ~70% dissolved, while the increased pH resulted in 100% precipitation for the 100 µM total Dy. This is likely an indication that at atmospheric CO_2, the amount of carbonate available for binding is the limiting condition affecting precipitation.

The addition of 1 mM total carbonate to the system substantially increased the amount of precipitation observed, especially at high pH. Again, the 1 µM total Dy data was found to be unreliable. However, the increased total carbonate concentration to 1 mM resulted in ~10-20% more precipitation at 10 µM total Dy for pH values 6 through 8, and 100% precipitation at pH 9. The increased total carbonate concentration showed a more obvious impact at 100 µM total Dy, as 100% precipitation was observed at all pH values, with the exception of the previously mentioned outlier at pH 7. Given that the ion product is proportional to the free Dy ion concentration and the carbonate concentration, it is logical that the increased C_T resulted in a higher probability of precipitation, particularly at the highest total Sm concentration. Since the total Dy concentrations studied are orders of magnitude below the total carbonate concentration in the system, it is likely that all free metal was complexed, leaving many carbonate ions free in solution.

The data observed at 10 mM total carbonate was very similar to what was observed at 1 mM C_T for all total metal concentrations and pH values. This indicates that the added sodium bicarbonate results in the dissolved carbonic acid species being in excess. Considering that the total Dy concentrations of interest were in the micromolar range, the amount of total metal available for binding several orders of magnitude less than the total carbonate concentration. Therefore, there is minimal change in the data despite the increase in total carbonate concentration.

3.3.3 The Role of Total Metal Concentration on Precipitate Formation

The total metal concentration present in solution can have a substantial impact on whether precipitation will occur. At low total metal concentrations, the metal is unlikely to precipitate in unfavourable conditions. With very little metal present in solution, precipitation is only expected at high ligand concentrations and/or high pH. However, at high total metal concentrations, metal species that are present in low fractions will still result in many ions in solution, thus providing an increased opportunity for binding.

3.3.3.1 Sm Results

Figure 3-9 below summarizes the data for % dissolved Sm vs SmT at fixed pH values of 6, 7, 8 and 9.

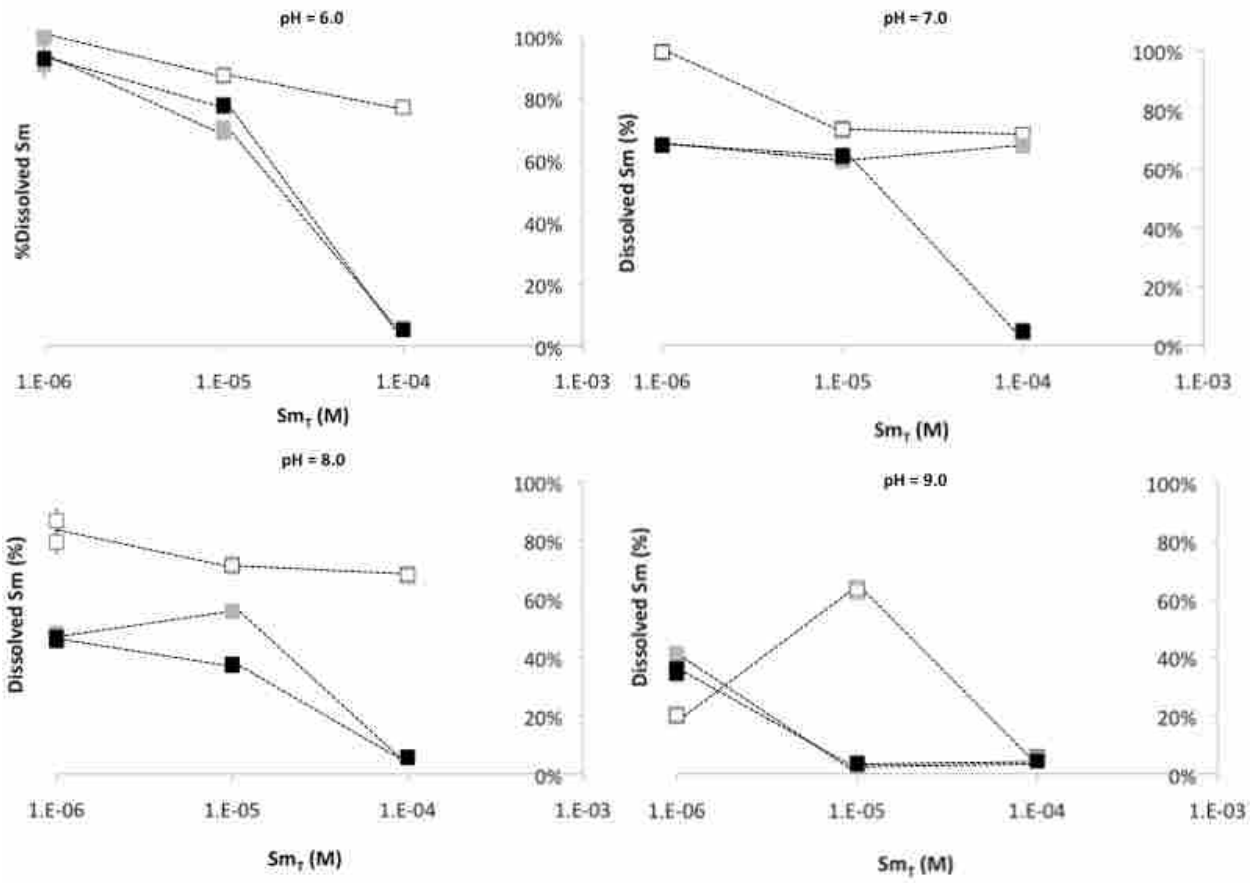

Figure 3-9: % dissolved Sm vs Sm_T at fixed C_T values of atmospheric CO_2, 1 mM and 10 mM and pH values of 6, 7, 8 and 9.
The experimental data show a decrease in the dissolved fraction with increasing total Sm concentrations, as expected.

At 1 µM total Sm, very little precipitation was observed, particularly at pH 6. At this low total metal concentration, the number of Sm free ions available for binding is minimal. While slightly more precipitation was observed at pH 7 and 8 with 1 and 10 mM C_T, only about 50% of the metal formed a precipitate.

At a concentration of 10 µM total Sm, a higher degree of precipitation was observed than at 1 µM, as expected. At pH values of 6 and 7, approximately 20-30% of the Sm precipitated. As the pH is increased to 8, 40% and 60% precipitation was observed for total carbonate concentrations of 1 mM and 10 mM, respectively. When the pH is increased to 9, 100% precipitation occurred for all total carbonate concentrations.

At an increased total Sm concentration of 100 µM, 100% precipitation was observed for all water chemistries containing total carbonate concentrations of 1 or 10 mM, with the exception of the outlier at pH 7. It is clear that at this total metal concentration, the system is saturated with dissolved Sm species that are available for binding.

In the study of trace metals like Sm, it is clear from the ion product expression for the formation of both hydroxide and carbonate precipitates that the free metal ion is the limiting component that affects precipitation. For this reason, precipitation typically occurs at the highest total metal concentration studied.

3.3.3.2 Dy Results

Figure 3-10 below summarizes the data for % dissolved Dy vs DyT at fixed pH values of 6, 7, 8 and 9.

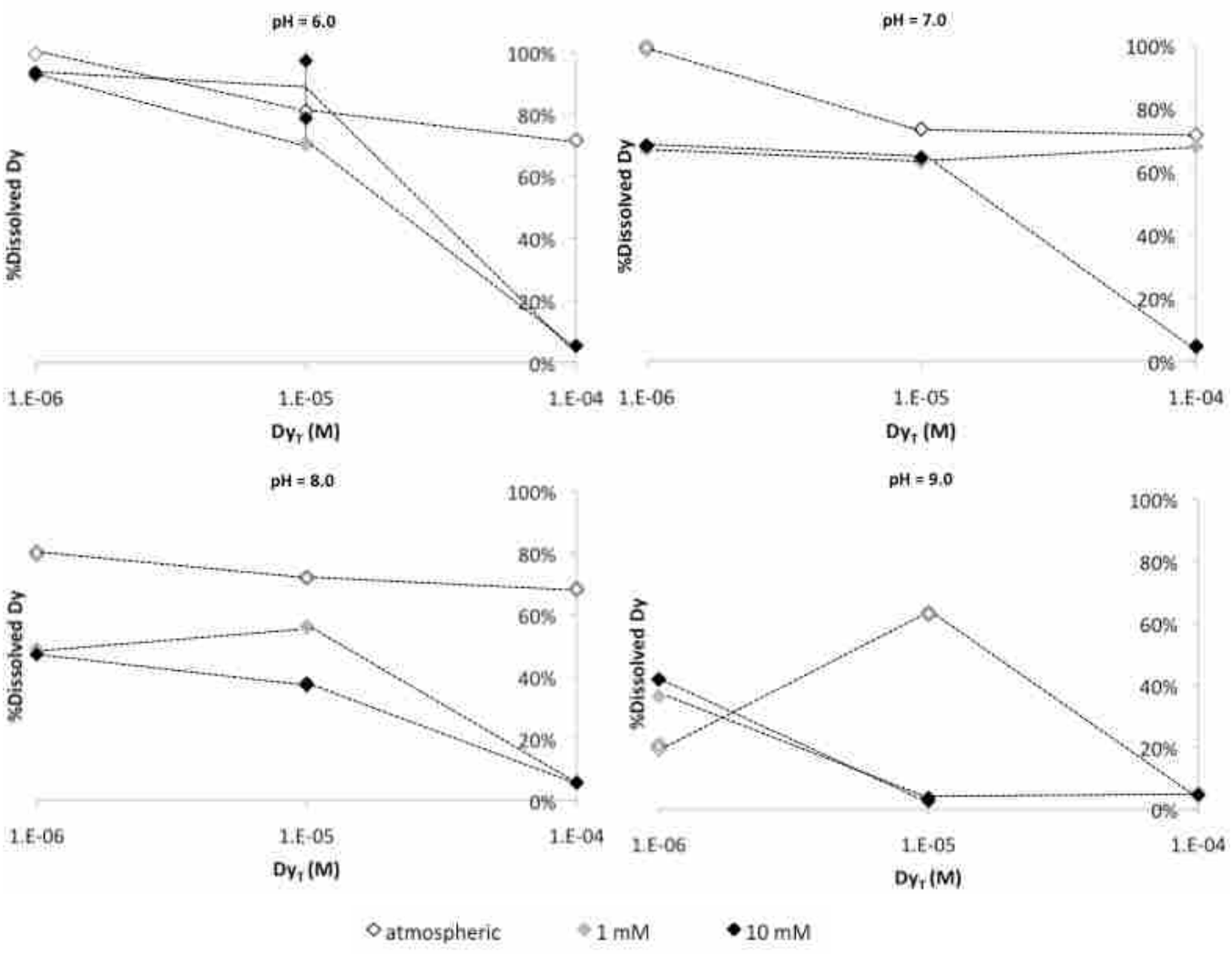

Figure 3-10: % dissolved Dy vs Dy_T at fixed C_T values of atmospheric CO_2, 1 mM and 10 mM and pH values of 6, 7, 8 and 9.
The experimental data show a decrease in the dissolved fraction with increasing total Dy concentrations, as expected.

At a total Dy concentration of 1 µM, very little precipitation was observed, particularly at pH 6. While increased precipitation was observed at pH 7 and 8, only about 30% and 50% precipitation occurred at these pH values, respectively. While slightly more precipitation was observed at pH 7 and 8 with 1 and 10 mM C_T, only about 50% of the metal formed a precipitate.

At a concentration of 10 µM total Dy, increased precipitation was observed for all pH values. At pH values of 6 and 7, approximately 20-30% of the Dy formed a precipitate. At an increased pH of 8, 40% and 60% precipitation were observed for total carbonate concentrations of 1 mM and 10 mM, respectively. When the pH was increased to 9, 100% precipitation occurred for all total carbonate concentrations.

At the highest total Dy concentration of 100 µM, 100% precipitation was observed for all water chemistries containing total carbonate concentrations of 1 or 10 mM, with the exception of the previously mentioned outlier at pH 7. At this total metal concentration, the system is saturated with dissolved Dy species that are available for binding. Therefore, in the presence of carbonate ions, precipitation is likely to occur.

In the study of trace metals such as Dy, the ion product expression for the formation of both hydroxide and carbonate precipitates indicates that the free metal ion is the limiting component that affects precipitation. For this reason, precipitation typically occurs at the highest total metal concentration studied.

4.0 Conclusions

The following conclusions were made based on the experimental results shown in chapter 3:

1. Experimental results obtained at a total metal concentration of 1 μM and/or atmospheric conditions were unreliable for two reasons
    a) Any metal lost to the walls of the container or sorption to the filter would represent a larger percentage of the total metal than at higher metal concentrations.
    b) Results obtained at this total metal concentration and/or low C_T are close to or below the instrumental detection limits of the ICP-OES used for measurements.
2. Steady-state conditions were achieved between the solid and liquid phases of the system within the first 24 h for all water chemistries with the exception of pH 9 and 100 μM total metal for both Sm and Dy. This is an indication that standard static acute toxicity 24-h renewals are suitable for most of the water chemistries studied. Therefore, I was successful in my completion of objective 1b).

    However, based on the decrease in dissolved fractions between 96 h and 120 h for many of the water chemistries studied, it does not appear that equilibrium was reached. This partially supports my hypothesis, as precipitation was expected to be slow. Unfortunately, based on the failure to reach equilibrium, I was unsuccessful in completing objective 1a) of developing better K_{sp} values using my solubility measurements.
3. Existing geochemical models do not agree that Sm and Dy behave uniformly.
    a) For Sm, geochemical models over predict precipitation for most water chemistries, with the exception of at low pH where no precipitation is predicted.
    b) For Dy, the opposite trend was predicted, with over predicted precipitation at high pH.

This information proves that existing geochemical models have been evaluated vs experimental data, as outlined in objective 2, and this objective was successfully completed.

4. Experimental results for 1 mM and 10 mM total carbonate concentrations agree strongly with one another for all total Sm and Dy concentrations. This is an indication that the Sm or Dy available for complexation, and therefore precipitation, is at a much lower concentration than carbonate.
5. All metal precipitates at pH 9 for most water chemistries for both Sm and Dy. Under these conditions, the system is saturated with both hydroxides and carbonates, providing a greater opportunity for precipitation.

Although there is insufficient data to develop a complete solubility model for Sm and Dy, conclusions 4 and 5 provide necessary information towards the use of solubility curves as a foundation for determining REE toxicity to pelagic aquatic organisms. However, objective 3 was not successfully completed.

5.0 Future Work

There is a substantial amount of future work that will be required in order to develop a complete and accurate solubility model for Sm and Dy.

First off, the formation of hydrolysis products needs to be explored for all pH values in order to investigate whether a U-shaped solubility curve exists for Sm and/or Dy, as it does for other trivalent metals. Current databases for geochemical modelling are conflicting about the formation

of hydrolysis products, specifically the fourth hydrolysis product, $Sm(OH)_4^-$ or $Dy(OH)_4^-$. Furthermore, as discussed in section 3.2.3, the Sm and Dy hydrolysis constants stated in the SKB database do not agree with one another, and Dy values do not follow the expected trend of hydrolysis constants for trivalent metals. It will be necessary for solubility experiments to be conducted at all pH values in order to verify documented hydrolysis constants and either confirm or refute the existence of the fourth hydrolysis product.

It would also be highly useful to explore the role that DOM plays on solubility. DOM exists in natural waters and acts as an organic ligand for metal binding. In freshwater, DOM competes with inorganic ligands such as hydroxide and carbonate to bind to Sm^{3+} and Dy^{3+} ions, and therefore reduces the amount of precipitation. This, in turn, increases their solubility. Future work should involve the completion of solubility experiments in the presence of DOM, in order to mimic the conditions under which precipitates would form in natural water. This would provide environmentally relevant solubility data.

Lastly, the SKB database used for geochemical modelling in this thesis predicts the existence of multi-ligand complexes for both Sm and Dy. However, K_{sp} values do not exist for these solids. Future work should involve the determination of whether these solids exist, what the corresponding formation constants are, and therefore the conditions under which they are likely to form.

6.0 References

Angel, B.M.; Apte, S.C.; Batley, G.E.; Raven M.D. Lead solubility in seawater: an experimental study. *Environ. Chem.* **2015,** *13,* 489-495.

Carroll, J.J. and Mather, A.E. The System Carbon Dioxide-Water and the Krichevsky-Kasarnovsky Equation. *J. Sol. Chem*. **1992**, *21*, 607-621.

Gimeno Serrano, M.J.; Auque Sanz, L.F.; Nordstrom, D.K. REE speciation in low-temperature acidic waters and the competitive effects of aluminum. *Chem. Geo.* **2000.** *165*, 167-180.

Gonzalez, V.; Vignati, D.A.L.; Pons, M.N.; Montarges-Pelletier, E.; Bojic, C.; Giamberini, L. Lanthanide ecotoxicity: First attempt to measure environmental risk for aquatic organisms. *Environmtl. Poll.* **2015.** *199*, 139-147.

Gustafsson, J.P. *Visual MINTEQ 3.1 User Guide.* **2014**.

Hem, J.D.; Roberson, C.E. Form and Stability of Aluminum Hydroxide Complexes in Dilute Solution. *U.S. Geological Survey – Supply Paper.* **1967.** *1827-A.* A1-A55.

Millero, F.J. Stability constants for the formation of rare earth-inorganic complexes as a function of ionic strength. *Geochimica et Cosmochimica Acta.* **1992.** *56*, 3123-3132.

Parkhurst, D.L. User's guide to PHREEQC--A computer program for speciation, reaction-path, advective-transport, and inverse geochemical calculations: U.S. Geological Survey Water-Resources Investigations Report. **1995**, *95-4227*, 143.

PerkinElmer User Manual. *Optima 8x00 Series ICP Optimal Emission Spectrometers*. **2013**.

Physical and Engineering Data, January 1978 ed. The Hague: Shell Internationale Petroleum Maatschappij BV, **1978**.

Reid, R.C.; Prausnitz, J.M.; and Poling, B.E. *The Properties of Gases & Liquids*, 4 ed. Boston: McGraw-Hill, **1987**.

Stefánsson, A. Iron(III) Hydrolysis and Solubility at 25°C. *Environ. Sci. Technol.* **2007.** *41*, 6117-6123.